Uncertainty of the peak flow reconstruction of the 1907 flood in the Ebro River in Xerta (NE Iberian Peninsula)

Josep Lluís RUIZ-BELLET[(a,*)], Xavier CASTELLTORT[(a)], J. Carles BALASCH[(a)], Jordi TUSET[(b,c)]

[(a)] Department of Environment and Soil Sciences, University of Lleida, Av. Rovira Roure 191, 25198 Lleida, Catalonia

[(b)] Forest Sciences Centre of Catalonia, Crta. Sant Llorenç de Morunys, km 2, 25280 Solsona, Catalonia

[(c)] RIUS Fluvial Dynamics Research Group, University of Lleida, Av. Rovira Roure 191, 25198 Lleida, Catalonia

[(*)] Corresponding author: jruizbellet@gmail.com

Abstract

There is no clear, unified and accepted method to estimate the uncertainty of hydraulic modelling results. In historical floods reconstruction, due to the lower precision of input data, the magnitude of this uncertainty could reach a high value. With the objectives of giving an estimate of the peak flow error of a typical historical flood reconstruction with the model HEC-RAS and of providing a quick, simple uncertainty assessment that an end user could easily apply, the uncertainty of the reconstructed peak flow of a major flood in the Ebro River (NE Iberian Peninsula) was calculated with a set of local sensitivity analyses on six input variables. The peak flow total error was estimated at ±31% and water height was found to be the most influential variable on peak flow, followed by Manning's n. However, the latter, due to its large uncertainty, was the greatest contributor to peak flow total error. Besides, the HEC-RAS resulting peak flow was compared to the ones obtained with the 2D model Iber and with Manning's equation; all three methods gave similar peak flows. Manning's equation gave almost the same result than HEC-RAS. The main conclusion is that, to ensure the lowest peak flow error, the reliability and precision of the flood mark should be thoroughly assessed.

Keywords: error; sensitivity analysis; Manning's roughness coefficient; DEM resolution; historical hydrology; hydraulic modelling

1. Introduction

Information about long-past floods, either in the form of paleostage indicators (sedimentary evidence) or historical documents, has in the last few decades begun to be used to reconstruct peak flow values. This approach reveals fruitful because the longer the time period considered, the greater the probability to include floods of extreme magnitude, which greatly enrich the information contained within the flood data series.

This relatively new branch of hydrology, subdivided in paleohydrology and historical hydrology (depending on the type of information used: paleostage indicators or historical documents) has suffered a great advance in the last decade (Bayliss and Reed, 2001; Benito et al., 2004, 2015; Brázdil et al., 2006; Elleder, 2010; Gaume et al., 2004; Naulet et al., 2005).

Different aspects of paleo- and historical hydrology have been investigated so far: the improvement and systematization of historical information data bases, the use of dendrogeomorphic evidences (Ruiz-Villanueva et al., 2010), the link between meteorological, hydrological and hydraulic processes (Bürger et al., 2006; Pino et al., 2015), or flood frequency analysis (Francés, 2004; Machado et al., 2015; Payrastre et al., 2011).

However, although one such important issue as the estimation of the uncertainty of the results of the hydraulic modelling has been deeply analysed (Lang et al., 2010; Neppel et al., 2010; Pappenberger et al., 2005, 2006), no clear methodological procedures as to its determination have been formulated. As a consequence, only a few historical flood reconstructions try to give an estimation of the uncertainty of the results (Herget and Meurs, 2010; Naulet et al., 2005; Remo and Pinter, 2007).

And yet, uncertainty is an essential part of the result, an attribute of information (Zadeh, 2005). As Johnson (1996) points out, if uncertainties cannot be determined, the results are inaccurate. Similarly, Beven (2006) thinks that not to estimate the uncertainty of a model prediction is “simply indefensible (or unscientific)” because hydrology is a highly uncertain science.

Actually, uncertainty in flow data is not negligible (Di Baldassarre and Montanari, 2009). Indeed, flow measurements with a current meter have errors between 5 and 20% (Léonard et al., 2000; Pelletier, 1988; Schmidt, 2002). Pappenberger et al. (2006) find that rating curve uncertainties cause an uncertainty of 18–25% in peak flow. Moreover, Lang et al. (2010) state that extreme flows uncertainties are larger than those of average flows. Thus, one should expect even larger uncertainties in historical hydrology reconstructions, where one has to model long-past extreme floods from a scarce set of data of sometimes unknown reliability, estimated rather than measured.

Götzinger and Bardossy (2008) and Refsgaard et al. (2006) identify three main sources of uncertainty in hydraulic modelling results:

- Uncertainties in the observations measurement. Some of them are:
    - Accuracy of the flood marks (Wohl, 1998).
    - Channel geometry and stream slope (Aronica et al. 1998; Jarret, 1987; Merwade et al., 2008; Pappenberger et al. 2005).
    - Viscosity of the fluid, affected by the amount of sediment load (Jarret, 1987).
    - Changes in the river bed morphology, either during the flood or between the flood and the date of the study due to erosion and sedimentation (Jarret, 1987; Lang et al., 2010; Wohl, 1998).
    - Representation of hydraulic structures such as bridges, culverts, and embankments (Merwade et al., 2008), their hydraulic behaviour and their being frequently blocked by debris and vegetation (Lang et al., 2010).
- Uncertainties in the parameters estimation, for example:
    - Accuracy of the Manning's n roughness coefficients (Jarret, 1987; Wohl, 1998).
    - Changes in the downstream boundary condition due to a back-water effect or to a hydraulic jump (Lang et al., 2010).
    - Expansion and contraction losses (Jarret, 1987).

- Uncertainty caused by end user’s decisions, the model structure (equations, hypotheses and assumptions), and the numerical methods used. Some of them are:
    - Number of cross sections, that is, spacing between cross sections (Jarret, 1987; Merwade et al., 2008).
    - Steady or unsteady flow (Jarret, 1987).
    - One-dimensional or two-dimensional modelling (Cea and Bladé, 2008).

Montanari (2007) distinguishes four types of techniques for assessing the uncertainty of hydrological modelling results; they can be also used in hydraulic modelling:

- Approximate analytical methods: e.g. first-order reliability method (FORM).
- Techniques based on the statistical analysis of model errors: e.g. Bayesian Forecasting System (BFS).
- Approximate numerical methods, that is, sensitivity analyses: e.g. the Generalised Likelihood Uncertainty Estimation (GLUE) methodology of (Beven and Binley, 1992).
- Non-probabilistic methods: e.g. fuzzy set theory.

In ungauged or scarcely gauged catchments (a frequent circumstance in historical hydrology), sensitivity analysis provides good uncertainty estimations (Montanari, 2007). Sensitivity is defined as a measure of the influence of the input variables on the result (McCuen, 1973). The existing types of sensitivity analysis have been reviewed by Van Griensven et al. (2006): the simplest of them is the local sensitivity analysis, in which each input variable of the model is separately modified at a time; another widely used type is the aforementioned GLUE methodology (Beven and Binley, 1992).

In spite of this profusion of methods and techniques, there is no unified procedure to guide hydrological and hydraulic modelling end users to easily quantify uncertainty (Merwade et al, 2008; Montanari, 2007; Pappenberger and Beven, 2006). Beven (2006) even wonders if these methods do not overestimate uncertainty.

The main objective of this article was to calculate the uncertainty of the resulting peak flow of a typical historical flood reconstruction with a simple and quick procedure of uncertainty estimation, one that an end user could easily apply. The secondary objective was to identify the input variables that influenced the result the most and their contribution to peak flow total error. The ultimate goal behind this secondary objective was to formulate some recommendations as to the degree of accuracy that each input variable should have in order to minimize results' uncertainty.

In order to achieve these objectives, the uncertainty of 1907 flood of the Ebro River in the town of Xerta (NE Iberian Peninsula) was calculated with a series of local sensitivity analyses of the main variables affecting the resulting peak flow; it must be noted that uncertainties stemming from model structure or numerical resolution methods were not analysed in this study. Besides, in order to see to what degree the result depended on the chosen model, the HEC-RAS resulting peak flow was compared to the ones obtained with the 2D model Iber and with Manning's equation.

5.2. Study area and study flood

The town of Xerta is located about 60 km upstream from the mouth of the Ebro River (Fig. 1). The Ebro River is one of the main rivers in the Iberian Peninsula. It drains into the Mediterranean Sea an area of 85,000 km^2, including almost completely the southern face of the Pyrenees. Its mean flow in Tortosa (13 km downstream Xerta) is 428 m^3·s^{-1} (Gallart and Llorens, 2004); since the average annual rainfall in the basin is 622 mm (period 1920–2000) and the basin area in Tortosa is 84,230 km^2, the runoff coefficient in that location is 25.8%.

[insert figure 1]

The climate within the basin is varied, ranging from wet Oceanic (Köppen Cfb) in some Pyrenean valleys to dry Mediterranean (Köppen Csa) in the centre of the basin. Floods in the Ebro River, with peak flows as high as ten times the mean flow in Tortosa, are more frequent in autumn and are usually caused by the two main tributaries Cinca and Segre, with headwaters in the Pyrenees.

Xerta (1250 inhabitants in 2014) is located on an ample floodplain by a meander of the Ebro River and opposite the town of Tivenys (Fig. 2); the Ebro basin in Xerta is 82,972 km^2 or 97.6% of its total area. The nearest gauging station is that of Tortosa (number 9027), which has been active since 1952; the highest instantaneous flow measured is 4580 m^3·s^{-1}, in 1961 (MAGRAMA, 2015). Xerta is a remarkable town in historical hydrology terms because it possesses a flood scale containing nine major floods since 1617 (Fig. 3), which have been hydraulically reconstructed by Sánchez (2007).

[insert figures 2 and 3]

The second highest of these floods, that of 21–23 October 1907, was selected to perform the uncertainty calculation for this article. This flood was caused by a rainfall episode that lasted three days and affected mainly the central Pyrenean area. The moderate rain depth fell on saturated soils, for only ten days before (12–13 October), an almost equally destructive (albeit somewhat smaller) flood had occurred (Balasch et al., 2007). The 21–23 October flood was the heaviest one in the Ebro basin in the 20th Century and ravaged many towns; some reconstructed peak flows and the destruction that this flood caused are shown in Table 1.

[insert table 1]

This flood was selected because it is a good case study of a major flood in the Ebro basin on which to explore different types of uncertainties associated to large floods hydraulic modelling. Besides, within the historical period, 1907 is a relatively recent year and, therefore, the input data required can be more accurately estimated. The 1907 flood is one of the floods with more flood marks along the Lower Ebro; because of that, it has been hydraulically modelled in different locations by Abellà (2013), Balasch et al. (2007), Mérida (2014), and Sánchez (2007). Besides, Pino et al. (2015) have included it in a comprehensive hydrometeorological analysis of 23 floods.

3. Methods

The process followed in this study had two parts (Fig. 4): On the one hand, the peak flow of 1907 flood in Xerta was calculated with three procedures: HEC-RAS (USACE, 2010a), Iber (Bladé et al., 2012), and Manning's equation; the three resulting peak flows were afterwards compared. On the other hand, the uncertainty of the peak flow obtained with HEC-RAS was assessed with sensitivity analyses. These analyses allowed us to determine the peak flow total error, the individual contribution of each tested input variable on that error and their individual influence on peak flow.

[insert figure 4]

3.1. Peak flow reconstruction of 1907 flood

3.1.1. HEC-RAS

The peak flow of 1907 flood was reconstructed in Xerta from the historical information available with the methodology of hydraulic modelling explained in Barriendos et al. (2014) and summarised in Fig. 5. It is important to note that the actual output of the hydraulic model used is water height, whereas the searched result was peak flow; therefore, the model was run iteratively with tentative peak flows until the observed water height was obtained. In any case, water height will be considered an input variable hereinafter.

Nowadays, there is a variety of hydraulic modelling programmes that can operate under different circumstances: either in steady or unsteady flow, and either in one dimension (that is, all flow lines are supposed perpendicular to the cross sections) or in two dimensions (flow lines are allowed to cross the cross section not perpendicularly). In this study, for the sake of simplicity, all calculations were performed with the widespread one-dimensional hydraulic modelling programme HEC-RAS, version 4.1 (USACE, 2010a). In steady, gradually varied flow, HEC-RAS uses the one-dimensional energy equation.

[insert figure 5]

The data used to model 1907 flood peak flow are shown in Table 2. Water height was obtained from the mark on the flood scale at 1, Major Square (Fig. 3); a secondary mark of the same 1907 flood located at 1, Major Street (60 m away from the first one) was used to assess the accuracy of the hydraulic modelling results.

[insert table 2]

The roughness coefficients (Manning's n hereinafter) of nine different soil uses were calibrated with 1961 (4 January) flood, of which there are a flood mark in Xerta's flood scale and a peak flow official measurement. This peak flow value was 4580 $m^3 \cdot s^{-1}$ in Tortosa (MAGRAMA, 2015) and was accepted for Xerta due to the short distance between both towns (13 km) and to the small difference in catchment area (1.5%). Soil uses were determined from aerial photographs of 1957 (ICGC, 2015) and were considered unchanged between 1907 and 1961 (Fig. 6). Indeed, an aerial photograph of

1927 (not used because of its low resolution) showed no changes between that date and 1957.

[insert figure 6]

The modelled reach consisted of 45 cross sections along 7690 m, that is, with an average distance between cross sections of 170 m. However, this distance was much smaller in the vicinity of the flood scale cross section, in order to obtain more accurate results (Fig. 7). The geometry of the channel and the floodplain was obtained from a Digital Elevation Model (DEM) with a horizontal resolution of 5x5 developed from LiDAR information of 2009 (IGN, 2015). This geometry, thus, was that of 2009; it was not modified to represent those of 1907 and 1961 because it was deemed stable and, therefore, with minimal changes throughout the period.

Indeed, the geometry can be considered stable both in the plan and cross section views. Aerial photographs since 1924 (the oldest ones from that area; aerial orthophotos since 1946 available at http://www.icc.cat/vissir3/) and the rocky bank upon which stands Tivenys (Figure 2) support the hypothesis of plan stability, whereas the conclusions of Vericat & Batalla (2006) support the hypothesis of the cross section stability. These authors claim that, since the construction of the dams upstream in the first half of the 20th century, the river bed in this area is subject to armouring due to high-frequency, low-magnitude floods, a fact that results in limited erosion.

In any case, we considered that, even if minimal changes in the cross sections geometry actually occurred, they did not imply a modification of the geometry variables used in the hydraulic modelling: longitudinal slope, wetted area and wetted perimeter. Indeed, in low-gradient reaches of large rivers very close to the sea such as Ebro River at Xerta, longitudinal slope is not controlled by local changes in cross section shape but by processes of much larger time- and space-scale, such as the base level, which has been stable in the last millennia; moreover, any relevant modification of longitudinal slope in such a low-gradient reach would have to affect a very long river stretch (about 100 km) in order to reach the equilibrium, which would imply the displacement of large quantities of sediment, an event that has not occurred between 1907 and 2009. Similarly, the wetted area and wetted perimeter of a given cross section may remain constant even if the cross section shape varies; indeed, along large cross sections such as the ones used in this model (from several hundred metres to more than one kilometre), changes of opposite sense (erosion and accretion) may occur simultaneously, thus cancelling each other out when the total wetted area or perimeter are calculated. And even if that were the case, its consequences over the modelled peak flow would be minimal: for example, if the river channel (150 m in length) suffered an incision of 1 m in the flood scale cross section (5060 m^2 in area), that would result in an increase of 150 m^2. When compared to the whole cross section, this area increase is 3%, which, even if we consider that water velocity in the channel doubles that on the floodplain, would translate into only a 6% increase in peak flow. This value is a very small error compared to the expected errors in historical floods' peak flow reconstruction (about 20-40%). Taking all these facts into account, we consider that the hypothesis of geometry stability since 1907 in the modelled reach is well supported.

[insert figure 7]

3.1.2. Iber

In a one-dimensional model such as HEC-RAS, the flow is always assumed to be perpendicular to each cross section. However, in floods over large floodplains, this assumption is no longer true: eddies, lateral and upstream flows, and backwater areas are common. One way to take this into account is to draw the cross sections with angulated segments (Fig. 8) instead of with a single straight line, in order that they be as perpendicular to the flow in each segment as possible. However, this does not completely solve the problem of modelling floodplain flow with one-dimensional models.

Thus, in the reconstruction of large floods that inundate wide floodplains with many obstacles such as buildings, 2D models, which allow for the horizontal component of the velocity vector, should provide a better estimation of the flow than 1D models (Cea and Bladé, 2008; Paquier and Mignot, 2003).

The 2D model Iber version 2.3.1 (Bladé et al., 2012) was used to obtain an alternative peak flow value, so as to quantify the difference and improvement obtained over a 1D model such as HEC-RAS. In order to enable the comparison between the results, the input data used were the same as for the modelling with HEC-RAS, including the Manning's n calibrated with HEC-RAS on 1961 flood, but excluding the specific parameters required in the 1D model (Table 2), and including others specific to Iber, such as the hydrograph shown in Table 3. Iber solves the 2D Saint Venant equations with the finite-volume method in unsteady flow.

[insert table 3]

3.1.3. Manning's equation

Hydraulic models, one- or two-dimensional, require some training and many data (namely, a Digital Elevation Model). Conversely, Manning's equation is a much simpler method to obtain the peak flow from a water height value. Thus, it was considered interesting to compare the results of the two previously presented computer-based hydraulic models with the result of the Manning's equation (Eq. 1) applied at the flood scale cross section.

$$Q = A \cdot \frac{1}{n} \cdot R^{2/3} \cdot s^{1/2} \qquad (1)$$

Where Q ($m^3 \cdot s^{-1}$): peak flow

A (m^2): wet area of the cross section at the moment of the peak flow

n ($s \cdot m^{-1/3}$): Manning's coefficient, related to the roughness of the cross section

R (m): hydraulic ratio of the cross section (wet area divided by wet perimeter) at the moment of the peak flow

S ($m \cdot m^{-1}$): longitudinal slope of the channel at the cross section

Actually, the flood scale cross section was divided in three different ways and Manning's equation was individually applied to each sector of each of the three methods of division; then, the peak flows of the individual sectors were added up. The three different resulting peak flows were averaged and compared to the ones obtained with HEC-RAS and Iber. The three ways in which the cross section was divided were:

- Division according to hydraulically homogeneous sectors: this resulted in five sectors (Fig. 9). Their characteristics, required to calculate Manning's equation, are shown in Table 4.
- Division according to soil use, using the same soil use map as in HEC-RAS and Iber modelling: this resulted in 17 sectors (Fig. 8). Their individual hydraulic characteristics are not showed.
- Division according to HEC-Geo-RAS, a programme that links a Geographical Information System (GIS) programme with HEC-RAS. HEC-Geo-RAS described the cross section with the coordinates of 277 points, resulting in 276 sectors (Fig. 8); their individual hydraulic characteristics are not showed.

[insert table 4 and figure 8]

3.2. Uncertainty assessment of HEC-RAS results

The uncertainty assessment of the peak flow obtained with HEC-RAS was done with a set of sensitivity analyses, technically called local sensitivity analyses, because they were performed separately on each selected input variable. In these analyses each input variable was varied within a range that was chosen either because it was considered adequate or because it was found in the literature. In any case, with the objective to obtain an upper boundary of peak flow uncertainty, the ranges of variation were chosen rather large. The hydraulic model was then run with the modified value of the input variable in order to obtain a new peak flow output. This new peak flow value was used to calculate the individual uncertainty of that input variable, that is, the variation of the peak flow caused by the individually modified input variable with Eq. (2a) when the variation was one-sided (i.e. only x+a or x–a) and with Eq. (2b) when the variation was symmetrical (i.e. x±a). Then, these individual uncertainties were added with a quadratic sum in order to obtain the peak flow total error (Eq. 3). The relative contribution of each variable to the peak flow total error was quantified with Eq. (4).

$$\delta_x = F_1 - F \quad \text{If variation of the variable is one-sided (only x+a or x-a)} \tag{2a}$$

$$\delta_x = \pm\left|\frac{(F_1 - F) + (F - F_2)}{2}\right| = \pm\left|\frac{F_1 - F_2}{2}\right| \quad \text{If variation of the variable is symmetrical (x±a)} \tag{2b}$$

$$\delta_{total} = \pm\sqrt{\sum_{x=1}^{n}[(\delta_x)^2]} \tag{3}$$

$$C_x = \frac{\delta_x}{\sum \delta_x} \cdot 100 \tag{4}$$

Where x: modified input variable in each individual sensitivity analysis n: number of modified input variables (or total sensitivity analyses)

δ_x ($m^3 \cdot s^{-1}$): individual uncertainty: variation of the peak flow caused by a variation in input variable x

δ_{total} ($m^3 \cdot s^{-1}$): total uncertainty of the peak flow

F ($m^3 \cdot s^{-1}$): peak flow obtained with the initial values of the input variable x

F_1 ($m^3 \cdot s^{-1}$): peak flow obtained with the modified value of the input variable x: x+a

F_2 ($m^3 \cdot s^{-1}$): peak flow obtained with the opposite modified value of the input variable x, when a symmetrical variation (x±a) was done: x–a

C_x (%): contribution of variable x to the total uncertainty of the peak flow

Besides, the results of the sensitivity analyses were also used to calculate a sensitivity index I_x for each varied input variable in order to determine to what degree each one affected the resulting peak flow (Eq. (5); adapted from Lenhart et al. 2002). This dimensionless parameter allows the identification of the most influential variables, regardless of the range within they are varied (Lenhart et al. 2002). According to the value of I_x, Lenhart et al. (2002) arbitrarily classify the influence of the input variable over the results as small or negligible ($|I_x|<0.05$), medium ($0.05\leq |I_x|< 0.02$), high ($0.02 \leq |I_x|<1$) or very high ($|I_x| \geq 1$).

$$I_x = \frac{\frac{F_1 - F_2}{F_{12}}}{\frac{x_1 - x_2}{x_{12}}} \quad (5)$$

Where I_x: sensitivity index of input variable x (dimensionless)

F_1 ($m^3 \cdot s^{-1}$): resulting peak flow when input variable x equals x_1 (x+a)

F_2 ($m^3 \cdot s^{-1}$): resulting peak flow when input variable x equals x_2 (x-a)

F_{12} ($m^3 \cdot s^{-1}$): resulting peak flow when input variable x equals x_{12}

x_{12}: mean of x_1 and x_2

Note: when the opposite modification of the input variable was not done (i.e. only x+a, instead of x±a), then F_2=0, x_2=0 and x_{12} is the initial value of variable x

The input variables upon which the sensitivity analyses were done were chosen from the list of the main factors affecting the uncertainty of hydraulic modelling results given in Sect. 1; these variables were: water height, Manning's n, downstream boundary condition, number of cross sections, direction of the flow paths, and horizontal resolution of the DEM. In total, 6 input variables were modified resulting in 14 different sensitivity analyses. Details of these 14 analyses, along with their results, can be found in the paragraphs below and in Table 8. Other variables that could have had an influence on the peak flow results, such as variations of the channel's geometry, the model structure or the numerical resolution methods, were not analysed, since the objective of the study was to perform a quick, simple uncertainty assessment. It must be noted that, Refsgaard et al. (2006) argue that model structure is the main source of uncertainty in model predictions, especially when extrapolating.

Flood marks signal the maximum height that the water reached during a flood. Many sources of error can contribute to the inaccuracy of the mark: the oscillating nature of the water surface of a flood, the time elapsed between the flood and the making of the mark, or even the capillary ascension of the water along the wall. In this study, water height was subject to three levels of symmetrical modification for the sensitivity analyses: ±10 cm, ±30 cm, ±100 cm, in order to represent three degrees of uncertainty. Uncertainty of the maximum water height obtained from a flood mark can be subdivided into two components: precision and reliability. Lang et al. (2010) estimate a precision of ±5 cm in water height measurements. Reliability, that is, the degree of truth that the flood mark conveys, can be affected by trivial but not so uncommon events such as inadvertently installing the flood mark plaque at a wrong height, either in a first moment, either after some restoration works (Benito et al., 2015); therefore, reliability must be assessed with historiographical methods that try to ascertain who, when, why and how marked the flood height (Barnolas and Llasat, 2007; Barriendos and Coeur, 2004; Bayliss and Reed, 2001). In other cases, the flood mark has no physical entity: it is not a plaque or a nick on a wall, but a written reference of a water height given in relation to a pre-existing object, such as a distinctive element in a bridge or a windowsill on a building's façade; in these cases, it is precision that is affected, because it is an indirect measurement and, thus, less accurate than the direct one given by a physical flood mark.In this study, it was decided that uncertainties greater than ±1 m would be related to extremely unreliable or imprecise historical sources and, therefore, not used in flood hydraulic reconstruction.

Marcus et al. (1992) found very high uncertainties for Manning's n: they found that Chow's (Chow, 1959) and Cowan's (Cowan, 1956) visual methods underestimated Manning's n from 28% up to 291% (141% in average) and from 21% up to 170% (100% in average), respectively. However, they tested these methods in conditions of extreme roughness: a steep glacier stream over coarse moraine sediment. Therefore, we chose a smaller range of variation for Manning's n (±30%), which is in the upper region of the range of typical uncertainty estimated for this variable by Johnson (1996):

±8–35%, and similar to the sensitivity analyses performed by Wohl (1998) and Casas et al. (2004): ±25%, Di Baldassarre and Montanari (2009): +33%, and higher than those of De Roo et al. (1996) and Naulet et al. (2005): ±20%.

Besides this modification of Manning's n (±30%), we also tested the accuracy of a simpler, more straightforward estimation of the roughness coefficients versus the highly elaborate and time consuming calibration done with 1961 flood and a detailed soil use map. Thus, a sensitivity analysis was performed in which the Manning's n of the channel was 0.045 $s \cdot m^{-1/3}$ and that of the floodplain was 0.056 $s \cdot m^{-1/3}$ regardless of the soil uses. These values were chosen because they are, in the case of the channel, the half-way point of the range given by Chow (1959) for this kind of river channel. In the case of the floodplain, Manning's n is the average of the half-way points of the ranges of the two prevailing soil uses in Fig. 6: crops and orchards and vegetated floodplain (shrubs), shown in Table 5. This average was not weighted by area, since it is supposed to be obtained from a perfunctory soil use determination.

Lang et al. (2004) suggest testing the influence on the peak flow result of different downstream boundary conditions and different hydrographs (under unsteady flow conditions), but they give no further instructions. This study was conducted with the normal depth chosen as the downstream boundary condition, because it is our usual procedure when no water depth and no flow are known downstream the modelled reach. When normal depth is selected, HEC-RAS asks the user a water surface slope. For the sake of simplicity, we considered the water surface parallel to the channel's bottom; therefore, 0.905 $m \cdot km^{-1}$, the longitudinal slope of the channel downstream the modelled reach, was introduced as the water surface slope (Table 2). The influence of the downstream boundary condition was assessed by varying this slope ±15%.

With regards to decisions that depend on the modeller's expertise, Paquier and Mignot (2003) stress the importance of correctly choosing the flow paths direction. Therefore, the influence of the drawing of the flow paths that HEC-RAS needs to operate, an arbitrary decision that depends on the expertise of the model user, was assessed. An initial, deemed more hydraulically correct, drawing located the flow paths over the floodplain in a more or less straight trajectory (Fig. 9a). A second drawing located the flow paths along the banks, following the meanders (Fig. 9b).

[insert figure 9]

The influence on peak flow of two more input variables was also assessed: the number of cross section (also a decision that depends on the modeller's expertise) and the horizontal resolution of the Digital Elevation Model (DEM). To do so, the model was run, on the one hand, with half the initial number of cross sections (22) by simply erasing every second cross section upstream and downstream the flood scale cross section, and on the other hand, with a much coarser DEM: with an horizontal resolution of 25x25 m (IGN, 2015) instead of 5x5 m.

4. Results and discussion

4.1. Manning's n calibration with the 1961 flood

The initial values of Manning's n –which had been used in the modelling of 1907 flood in Móra d'Ebre (40 km upstream) by Abellà (2013)– were calibrated using the known peak flow of 1961 flood (4580 $m^3 \cdot s^{-1}$) and its associated observed water height (recorded in the flood scale and shown in Table 2). Thus, the Manning's n were modified until the difference between the observed and the modelled water heights was only 1 mm. This calibration dramatically improved the model's accuracy because, if the Manning's n values before the calibration (which were 2.3% higher in average, but 16% smaller in the channel) had been used instead, the resulting peak flow for 1961 would have been 5260 $m^3 \cdot s^{-1}$; that is, 13.8% higher than the actual measured peak flow. The longitudinal water profile obtained with the calibrated model is shown, in Figure 10, along with the flood mark used.

The calibrated Manning's n were within the ranges given by Chow (1959) and, except for two soil uses (vegetated floodplains and urban area), they were quite similar to those calibrated by Sánchez (2007) with the same flood in the same reach (Table 5). The greater difference with Sánchez was in the urban area: the high value we used accounts for the zigzagging trajectories that water has to follow when flowing through the town streets, which slow it down. These discrepancies, although important, fall within the range of uncertainties given by Marcus et al. (1992) for Manning's n determination with Chow's visual method (28–291%). Nonetheless, they illustrate the difficulty to objectively estimate the roughness coefficients, even when they can be calibrated with the same known flow. In any case, the positive differences in individual soil uses compensated almost completely the negative ones, as shown by the relative difference in the Manning's n averaged by the area of each soil use within the flooded part of the modelled reach: –20%.

[insert table 5]

The channel's Manning's n found is considerably higher than the ones calibrated in the same Ebro River with the same 1961 flood by Mérida (2014) in Benifallet (12 km upstream) and Abellà (2013) in Móra d'Ebre (40 km upstream Xerta): 0.024 and 0.028. Our higher value, as well as the one found by Sánchez (2007), can be explained by the extra roughness provided by the double meander on which Xerta lies (Fig. 9).

4.2. Peak flow reconstruction

4.2.1. HEC-RAS

Figure 10 shows the modelled longitudinal water profile of 1907 flood along the reach and the two flood marks used. The reconstructed peak flow of 1907 flood in Xerta was 11500 $m^3 \cdot s^{-1}$, which gave a modelled water height only 0.5 cm below the mark in the flood scale (Table 6). The goodness of this result is furthermore confirmed by the small difference between modelled water height and observed water height at Major Street's flood mark: 0.5 cm. Besides, the resulting peak flow is close to (and, thus, coherent with) the ones calculated with HEC-RAS in Móra d'Ebre (40 km upstream) by Abellà (2013) and in Benifallet (12 km upstream) by Mérida (2014): 11200 and 11500 $m^3 \cdot s^{-1}$, and to the one estimated by López-Bustos (1972) in Tortosa (13 km downstream):

12000 $m^3 \cdot s^{-1}$ (Table 1); relative differences with our result are less than 3%, 0% and 4% , respectively.

[insert table 6]

The difference with the peak flow calculated by Sánchez (2007) with HEC-RAS in Xerta (10500 $m^3 \cdot s^{-1}$) is a little bit greater: 9%. In any case, this amount of difference is acceptable in historical hydrology and smaller than the peak flow total error presented in Sect. 4.3 (±31%). Probably, the different peak flows are due, on the one hand, to the 20% difference in Manning's n (Table 5) and, on the other hand, to the smaller cross section that Sánchez used in the town, caused by his decision to consider the whole urban area (not only the buildings, but also the streets) hydraulically ineffective, that is, to consider that water did not flow across that part of the section. This decision results in his effective cross section at the flood scale being 16% smaller than ours (4675 m^2 and 5504 m^2, respectively). These differences illustrate the relative insensitivity of hydraulic modelling results: the combined effect of a 20% increase in Manning's and a 16% reduction in cross section area was only a 9% reduction in peak flow. Most likely, this insensitivity is caused by the fact that the reduction of cross section area affected a section were the flow was low, due to the low water stage and the high friction.

[insert figure 10]

4.2.2. Iber

The value of the peak flow reconstructed with the two-dimensional hydraulic model Iber was 12000 $m^3 \cdot s^{-1}$, that is, 4% higher than the one reconstructed with the one-dimensional model HEC-RAS. This small difference, much smaller than the total error presented in Sect. 4.3, confirms the validity of the reconstructed peak flow.

This coincidence of results contrasts with what Mérida (2014) finds in a similar comparison of the two models for the same 1907 flood in Benifallet (12 km upstream Xerta): 11300 $m^3 \cdot s^{-1}$ with HEC-RAS and 10000 $m^3 \cdot s^{-1}$ with Iber, or a difference of 12%. He also finds that Iber is much less sensitive to Manning's n; however, he suspects that the low sensitivity of Iber's results is due to the fact that the rating curve, required as a boundary condition in Iber, is left unchanged. Our coinciding results also contrast with the accepted fact that 2D are more accurate than 1D models, especially in floods over large floodplains (Cea and Bladé, 2008; Paquier and Mignot, 2003;).

In any case, two-dimensional models will only yield more accurate results than one-dimensional ones if they are fed very detailed input data (Merwade et al., 2008). Certainly, Lang et al. (2004) obtain a larger peak flow error (40%) with a 2D model than with a 1D model in the Onyar River in Girona because parameter calibration is more difficult. Moreover, under conditions of abundance of data to perform a complete calibration, Horritt and Bates (2002) find that HEC-RAS results are as good as the 2D model TELEMAC-2D in a 60 km reach of the Severn River. Therefore, no clear conclusions about the superiority of 2D models with respect to 1D ones can be drawn.

4.2.3. Manning's equation

The three resulting peak flows using Manning's equation in the three divisions on the flood scale cross section were: 11172, 11534 and 11759 $m^3 \cdot s^{-1}$ (Table 7). Their average was 11488 $m^3 \cdot s^{-1}$ and their standard deviation, ±296 $m^3 \cdot s^{-1}$ (±3%). This result coincides with the peak flow we calculated with HEC-RAS: relative differences are, respectively 3%, 0% and 2%.

[insert table 7]

In conclusion, the calculation of the peak flow of 1907 flood in Xerta with Manning's equation seems to produce acceptable results with an easier method than computer-based hydraulic models. However, the lack of a peak flow error makes it impossible to compare the accuracy of the three methods used: HEC-RAS, Iber and Manning's equation. Certainly, if the total error of the peak flow calculated with Manning's equation were too large, there would be no advantage in using that method.

In any case, Harmel et al. (2006) report uncertainties in peak flow estimation with Manning's equation from ±15%, in stable, uniform channels with an accurately estimated n, up to ±35%, in unstable, irregular channels, with poorly estimated n; these are totally acceptable peak flow errors. Herget et al. (2014) have reconstructed 15 peak flows in six locations with Manning's equation, with results that underestimate the referential gauged values from 4% to 9% in ten cases and from 16% to 28% in the other five. This systematic underestimation of peak flow with Manning's equation with respect to gauged values in large river floods contrasts with the frequent overestimation that Lumbroso and Gaume (2012) observe, although, in their case, in flash floods; they also find much larger peak flow errors in flash floods hydraulic reconstruction (±50%), which they consider caused almost solely by errors in Manning’s n estimation when done by visual methods.

Although a sensitivity analysis of Manning’s equation was not done, the three slightly different peak flows obtained with the three methods of dividing the cross section are a sign of the sensitivity of the results using Manning’s equation. For example, Herget and Meurs (2010) and Herget et al. (2015) find sensitivity indexes of the roughness coefficient between –0.9 and –1.1, slightly above the ones found with HEC-RAS in other studies (Table 10).

4.3. Uncertainty assessment of HEC-RAS results

Table 8 shows the results of the 14 sensitivity analyses performed. According to the sensitivity indexes obtained, water height is the most influential input variable over peak flow. Manning’s n comes next, followed by the number of cross sections and the downstream boundary condition; the other two variables (flow paths direction and DEM resolution) have much less or no influence on peak flow results.

[insert table 8]

Peak flow total error was calculated with Eq. (3). Actually, it was calculated combining different water height uncertainties with the fact of taking or not taking into account the error caused by the reduction of the number of cross sections (Table 9). In fact, it is very rare for a modeller to use too few cross sections, since there are clear recommendations about that and the HEC-RAS model displays alerts when this occurs; therefore, and considering that the flood scale is very precise and reliable, the total relative error of the reconstructed peak flow of 1907 flood in Xerta was 31%. But even if the flood mark were a lot less precise, the total error would not increase excessively: ±39%.

[insert table 9]

These errors are comparable to that obtained for extreme floods by Naulet et al. (2005) in the Ardèche River: +40%, and to those that we estimated in Ruiz-Bellet et al. (2015) in six flash flood reconstructions: ±5–44%, and totally acceptable in historical hydrology. Indeed, Neppel et al. (2010) estimate that the uncertainty of the peak flows of extreme floods calculated with rating curves lies in the range of 10–100% and Cong and Xu (1987) consider that information about large floods is useful even with errors up to 60%. For comparison, Pelletier (1988) estimates the error of a good flow measurement at 5%.

4.3.1. Water height

Water height uncertainty is the most influential input variable over peak flow results; in fact, it is 3.6 times more influential than Manning's n (Table 8). This agrees with Lang et al. (2010), who find that a variation of a few dozen centimetres in water stage in a wide river (10–50 m) cause large uncertainties in the estimated flow.

In the case of 1907 flood in Xerta, the relationship between water height uncertainty and peak flow relative error is very lineal: each ±10 cm of uncertainty in water height causes a relative error of ±2.4% in peak flow (Fig. 11). In Ruiz-Bellet et al. (2015), we found slightly higher relationships between peak flow errors and water height uncertainty: between ±3% and ±14% for each ±10 cm, in six hydraulic reconstructions of flash floods in streams with small basins (between 56 and 314 km^2).

[insert figure 11]

It must be noted that, although water height is the most influential input variable over peak flow results, it is not the major contributor to peak flow total error: Manning's n and, when included in the calculations, the number of cross sections contribute more to the peak flow total error (Table 9). In fact, this contribution depends, on the one hand, on the influence of the variable (measured by its sensitivity index) and, on the other hand, on the magnitude of its own uncertainty. Manning's n, with its ±30% uncertainty, is a much bigger contributor to total error in spite of being somewhat less influential. This analysis permits to visualise the magnitude, of a ±30% uncertainty in Manning's n: it is a great uncertainty, even greater than ±100 cm in water height in terms of contribution to peak flow total error. However, as explained in Sect. 3.2, this great uncertainty is a reasonable value, due to the fact that it is a very difficult variable to determine in absence of water height and flow measurements. The same reasoning can be done with the number of cross sections: its sensitivity index (thus, its influence over the result) is lower than that of water height, but its modification (that is, its uncertainty) is greater: from 45 to 22 cross sections or a reduction of 50%; however, in the cross section case, unlike in the Manning's n, this extreme variation seems less likely to occur in the practical application of a model and was only tested for theoretical purposes.

4.3.2. Manning's n

Manning's n is the second most influential variable over peak flow results, with a sensitivity index of –1.0, classified as very high by Lenhart et al. (2002); in any case, it is similar or slightly higher than others found in the literature (Table 10). Manning's n is, as said in Sect. 4.3.1., a major contributor to peak flow total error due to its high uncertainty. Certainly, an error of ±30% in determining Manning's n, which is a relatively high but not uncommon value (as specified in Sect. 3.2), caused an error of ±30.4% in 1907 flood's peak flow in Xerta.

[insert table 10]

Manning's n is a difficult variable to estimate, since it depends on many factors, such as the channel and floodplain geometry, the roughness of their surfaces, the type and abundance of riverine vegetation, or even the characteristics of the flow. Therefore, it is somewhat subjective and very dependent on the experience of the technician in the studied area. That is why we assigned a high error to it. More precisely, in our sensitivity analysis, we modified the Manning's n of all the soil uses in all the cross sections exactly in the same amount and sign: either +30% or –30%. This kind of systematic error seems quite improbable. Rather, Manning's n would be underestimated in some cross sections and overestimated in others within the modelled river reach, thus ones compensating others. Therefore, and taking also into account that ±30% is quite a relatively generous uncertainty for Manning's n, our estimation seems to be an upper boundary of the uncertainty in the resulting peak flow caused by that input variable.

Wohl (1998) concludes that the influence of Manning's n is greater in steep, narrow, and highly rough channels, than in flatter, wider, smoother ones. Wohl's conclusion is in contradiction with Dawdy and Motayed (1979) and O'Connor and Webb (1988), who find that the Manning's n has a small influence on peak flow results when using HEC-2, a precursor of HEC-RAS, in deep, narrow channels.

Similarly, Chow (1959) states that Manning's n influence is greater in low flows than in high flows; this concurs with the findings of Naulet et al. (2005): in their modelled reach of the Ardèche River, a change of ±20% in Manning's n results in a change of ±20% in the peak flow of medium floods and of ±10% in large floods, this being explained by the reduced effect of roughness in flows with high depths. This conclusion also agrees with what we found in Balasch et al. (2011): for low flows, a decrease of 50% in Manning's n causes no variation in peak flow, but a 10% increase in n causes a 7% decrease in peak flow, which is larger than the 1.5% caused by the same variation of n in high flows.

Hall et al. (2005) find that the channel Manning's n is the factor that influences the most the model's results in a reach of the River Thames in the United Kingdom, but that floodplain Manning's n gains importance in the wider parts of their modelled reach, where there is more out-of-bank flow. Similarly, Alemseged and Rientjes (2007) find that channel's Manning's n values affect more the resulting peak flow than floodplain values and Schumann et al. (2008) find that floodplain Manning's n has no influence on hydraulic modelling results when varied between 0.04 and 0.1 $s \cdot m^{-1/3}$ in their modelled flood. In this study, the separate effects on the peak flow of the roughness of the channel and the floodplain were not assessed. However, when calibrating the Manning's n with 1961 flood, channel's roughness coefficient seemed to be more influential than those of the floodplain. Nevertheless, there was much less overbank flow in 1961 than in 1907 and, therefore, no conclusion can be drawn about which segment's roughness (channel or floodplain) affects the most the peak flow of an extreme flood such as that of 1907.

Casas et al. (2004) find that Manning's n has a greater influence on the modelling results as the resolution of the DEM increases; in other words, a hydraulic model run on a coarse DEM is less sensible to uncertainties in Manning's n than when run on a finer one. This kind of interaction between input variables over peak flow results was not analysed in this study.

In this study, Manning's n were determined, as explained in Sect. 3, with a lengthy procedure involving soil use mapping from old aerial photographs and a calibration with 1961 flood. However, in spite of its complexity, it gave, for some soil uses, very different estimations than the same method applied by Sánchez (2007) to the same reach and calibrated with the same flood (Table 5). It was therefore thought interesting to test the accuracy of a more straightforward determination of the roughness coefficients. In this determination, the channel was assigned a Manning's n of 0.045 $s \cdot m^{-1/3}$ and the rest of the flooded area, 0.056 $s \cdot m^{-1/3}$. This resulted in a Manning's n, averaged by area, of 0.053 $s \cdot m^{-1/3}$, that is, an increase of 8% with respect the initial average Manning's n: 0.049 $s \cdot m^{-1/3}$. This reduction is contained within the previous ±30% variation; therefore, the individual error on peak flow that it caused was not included in the calculation of the total error (Table 9).

This increase of 8% in the average Manning's n produced a decrease of 11% in the peak flow (10225 $m^3 \cdot s^{-1}$) and, thus, a sensitivity index of −1.4 (sensitivity analysis 9 in Table 8), only slightly higher than the one found with the variation of ±30% (sensitivity analyses 7 and 8 in Table 8).

In any case, a perfunctory determination of Manning's n resulted in an average value only 8% larger than the one obtained after a long, detailed procedure. This error in Manning's n is smaller than the one considered in the uncertainty assessment (±30%). Therefore, it seems, at least in this case, that an extremely accurate determination of Manning's n is not cost-effective. This conclusion is in contradiction with the previous statement that Manning's n is the second most influential variable over the results: if it is so influential, it should be accurately determined. Actually, if in a peak flow uncertainty assessment, the assigned uncertainty to Manning's n is large (as it is advisable to do due to the difficulty in determining it), there is no need to accurately estimate it. A parallel with water height can help to explain this idea: to measure an unreliable flood mark to the μm would be a loss of time, because its uncertainty can be up to ±100 cm.

This conclusion of the limited influence of the estimation method on Manning's n accuracy is in disagreement with the findings of Ghani et al. (2007). Indeed, they report a reduction in discharge error from +200% to ±10% when the method for estimating Manning's n is changed from a ready-to-use one to a custom-made one. A possible reason of this discrepancy with our findings may be the different magnitude and nature of the discharges: a peak flow of 11500 $m^3 \cdot s^{-1}$ during an extraordinary flood in the Ebro River, against ordinary discharges of 3 to 88 $m^3 \cdot s^{-1}$ in the three small Malaysian rivers.

4.3.3. Downstream boundary condition

Peak flow results are moderately sensitive to variations of the boundary condition set 2700 m downstream (sensitivity index of +0.3; Table 8). This contrasts with Alemseged and Rientjes (2007), who conclude that the effects of the boundary conditions are significant only near the downstream end of the river reach. However, Naulet et al. (2005) find, in a reach of the Ardèche River with a slope of less than 2.5 $m \cdot km^{-1}$ modelled with the MAGE hydraulic model, that a variation of ±1 m in the downstream condition has effects in the peak flow as far as 12 km upstream.

4.3.4. Number of cross sections

When running the model with half the initial number of cross sections (22), the resulting peak flow was 25% higher than with all 45 cross sections. This variable has a relatively high sensitivity index (0.5) and, due to the wide range of variation of its local sensitivity analysis (-50%), it has a high contribution to the peak flow total error (between 29% and 40%) if included in the calculation (which, as said in Sect. 4.3, does not seem necessary because the HEC-RAS model has an automatic warning system that alerts when too few cross sections are being used), ,.

Alemseged and Rientjes (2007) find that different cross section spacing (2 to 20 m) results in different water surface profiles, only near the downstream end of the modelled river stretch. Cea and Bladé (2008) suggest placing the cross sections in representative spots within the modelled reach, spaced between 1 and 5 times the reach's width. They warn against an excessive number of cross sections, since this could cause errors in the model's iterative calculation process. The effect of an excessive number of cross sections and of their exact location along the reach has not been analysed in this study.

4.3.5. Flow paths

The results show that, in the case of 1907 flood in Xerta, the direction and location of the flow paths has no influence on the peak flow results.

4.3.6. DEM horizontal resolution

To use a lower resolution DEM (25x25 m instead of 5x5 m) resulted in a practically no change of the initially modelled peak flow: a reduction of 0.2%. Certainly, the influence of this variable on peak flow is very small: its sensitivity index is 0.01; and its relative contribution to total peak flow error is also reduced: less than 1%. These results seem to agree with Horritt and Bates (2001), who find that, when modelling a flood of the River Severn with the 1D model LISFLOOD-FP and its NCFS version, a resolution of 500x500 m is adequate enough and resolutions finer than 100x100 m do not further improve the results. However, our results are in contradiction with various studies, which have shown that small errors in the topography can have significant effects on model results (Bates et al., 1997; Nicholas and Walling, 1998; Wilson, 2004) and with other studies that even conclude that the representation of the channel geometry seems to be the most influencing aspect of hydraulic modelling (Aronica et al. 1998; Merwade et al., 2008; Pappenberger et al. 2005). Similarly, Casas et al. (2004) conclude that a HEC-RAS model run on coarse-resolution DEM produces lower peak flows than when run on finer DEM, and that this difference is greater for low flows than for high flows. Alemseged and Rientjes (2007) also find, although in a two-dimensional model, that reducing the DEM resolution causes a reduction of water velocity (and, therefore, of peak flow).

4.3.7. Input variables not analysed

The peak flow total errors shown in Table 9 include variables the error of which can be easily reduced, such as the drawing of flow paths, the number of cross sections and the resolution of the DEM. One could think that this gives an upper bound of the total uncertainty of the modelled peak flow. However, the set of sensitivity analyses performed is far from being exhaustive and other input variables not taken into account could increase that total error.

The influence of those input variables was not quantified in this study because their analyses were deemed too difficult to be included in a basic uncertainty assessment intended for an end user, which was the main objective of this article. In any case, a short discussion of other studies' findings is provided below.

4.3.7.1. Channel's erosion and accretion

The erosion and accretion of the channel, either during the reconstructed flood or between the date of the flood and that of its reconstruction, can cause significant changes in the geometry than can ultimately translate into errors in the hydraulic modelling results.

According to Kirby (1987), erosion is of extreme importance in modelling. Actually, Sauer and Meyer (1992) find that a mobile, unstable bed can cause an error of 10% in water stage measurement. Similarly, Naulet et al. (2005) find, in a modelled reach of the Ardèche River, that variations of –4/+2 m in the river bed height result in a variation of ±7% in peak flow for medium floods and of ±10% for extreme floods. However, Balasch et al. (2011) obtained the same peak flow when modelling a flash flood with two different channel geometries.

4.3.7.2. Sediment transport

Sediment transport, a factor rarely taken into account, can alter the hydraulic modelling results. In fact, according to Quick (1991), in floods with an important sediment transport, one third of the hydraulic energy is consumed in conveying the sediment and the other two thirds in moving the water. Therefore, not taking into account sediment load tends to overestimate peak flow.

But this overestimation can be even greater when hyper-concentrated flows occur, because then the fluid ceases to be Newtonian and the equations used by the model no longer apply. Although this is an infrequent circumstance in river flows such as 1907 in Xerta, it is not uncommon in flash floods in scarcely vegetated catchments: for example, Balasch et al. (2010a), report a sediment volume of 12% in one historical flood, which would qualify as a hyper-concentrated flow.

4.3.7.3. Steady and unsteady flow

One of these non-analysed input variables is the choice between steady and unsteady flow. In this study, the steady flow was used because it needs less information or, in the lack of it, less assumptions. However, steady flow is thought to overestimate the peak flow, since it does not allow for water storage over the floodplain. Actually, Naulet et al. (2005) find that the steady flow condition overestimates extreme floods' peak flows by 2%, in a modelled reach of the Ardèche River; similarly, Tuset (2011) finds an overestimation of 8% in the reconstruction of a flash flood in a 220 km^2 catchment. Besides, Bales and Wagner (2009) state that the effect on the results of modelling with a steady flow is greater for high flows than for low flows because water storage over the floodplain is greater. Nevertheless, this effect is diminished in floods with a prolonged, stable peak flow (that it, with a flat-summited hydrograph), virtually equivalent to a steady flow.

In any case, choosing the unsteady flow option in the HEC-RAS model does not automatically reduce the uncertainty of the results. Indeed, the unsteady flow choice requires a hydrograph and Alemseged and Rientjes (2007) claim that the shape of that hydrograph affects the hydraulic modelling results, although not significantly.

5. Conclusions

The peak flow of 1907 flood in the Ebro River in Xerta, reconstructed with HEC-RAS, was 11500 $m^3 \cdot s^{-1}$ and its total error was ±31%. However, actual total error could be greater because the uncertainty assessment did not include other possible sources of error, such as geometry modifications of the channel due to erosion and sedimentation or model structure. Anyway, the assessment procedure used proved to be a quick, simple one that obtained a rough but reliable estimate of peak flow error, similar to the values found in the literature.

The most influential input variable over peak flow results was water height; however, the one that contributed the most to peak flow error was Manning's n, because its uncertainty was far greater than water height's. The drastic reduction of the number of cross sections resulted in a great variation of peak flow; however, since there are clear recommendations regarding the minimal number of cross sections needed in a modelled reach, such an extreme scenario seems improbable to occur. The other three analysed variables (downstream boundary condition, flow paths direction, DEM resolution) had far less influence on both the peak flow and its uncertainty.

A simple, straightforward method of determining Manning's n provided roughness coefficients similar to the ones obtained with a more convoluted method that included a detailed soil uses mapping and a calibration with a known peak flow.

In view of all this, it would be advisable, when attempting the hydraulic reconstruction of a historical flood, to soundly verify the reliability of the flood marks and, afterwards, to precisely measure them, since water height is the input variable that most influences the results. Conversely, Manning's n estimation does not need to be extremely accurate, since the methods to do so are often subject to strong uncertainties; in other words, thorough estimations are not necessarily closer to the actual roughness coefficients values than more cursory ones. The quantification of the other tested variables does not need to be extremely precise either, since they have even less influence over the modelling results.

In order to reduce the inherent uncertainty of a hydraulic reconstruction, several sensible steps should also be taken when possible:

1) To use more than one flood mark along the modelled river reach in order to obtain a more accurate water profile.

2) To assess the evolution of the river’s channel and flood plain morphology, in order to reduce the uncertainty contributed by this factor.

3) To calibrate the hydraulic model with measured flows of more modern extreme floods.

4) To reconstruct the flood in several locations throughout the basin in order to validate the results reciprocally through discharge continuity along the river.

As said above, the uncertainty assessment did not include all the variables that could affect the peak flow error. An improved uncertainty assessment with the objective of calculating the upper bound of the actual peak flow total error should include all the possible sources of error, as well as interactions between them (that is, the influence of simultaneous modifications of different variables). These interactions need to be analysed with a global sensitivity analysis instead of with a collection of local ones. In order to do so, and also in order to apply other uncertainty assessment procedures such as the GLUE (Beven and Binley, 1992), the introduction of input variables into the model should be automated, due to the high number of simulations needed.

Nonetheless, a totally complete quantification of peak flow uncertainty seems very difficult. Indeed, the use of a hydraulic model implies a great number of small decisions that depend on the modeller’s expertise or, in other words, that convey a small amount of subjectivity. These decisions cannot be all taken into account in an uncertainty assessment, but can cause great differences between the results of two different modellers.

Furthermore, a thorough comparison between 1D and 2D models could be done in order to determine if the more complex to operate two-dimensional programmes are actually more accurate while still being cost-effective when calculating peak flow in wide floodplains with many obstacles to the flow. Besides, more research is needed to ascertain if the channel's Manning's n is more influential on peak flow than the floodplain's.

The simple method of applying Manning's equation at a single cross section seems to yield acceptable results, very similar to the one obtained with the HEC-RAS model. However, an uncertainty assessment is needed in order to compare its accuracy to that of computer-based methods.

This study was limited to peak flow uncertainties; however, the uncertainties of other hydraulic modelling results relevant to in flood risk management, such as the flooded surface or the flood wave travel time, could also be assessed.

The method of error assessment for historical floods reconstruction used in this paper can be convenient for end users because it is extremely simple, which has two consequences: it provides a quick but sound estimation of the modelled peak flow error –a critical piece of information often absent in technical reports– and it does not require a great command of complex statistical techniques as other methods, more oriented to specialised scientists, do. Moreover, this method quantifies the weight of each input variable in the peak flow total error, thus allowing the end user to decide which need to be more precisely determined to reduce that error.

Acknowledgements

Damià Vericat drew the map in Fig. 1c. Alberto Sánchez measured the heights of the three flood marks used in this study (Table 2) and took the photo in Fig. 3.

We thank Ramon J. Batalla (RIUS-UdL), Andras Bardossy (editor of Journal of Hydrology), Gerardo Benito (CSIC), Michel Lang (IRSTEA), Ralf Merz (editor of Journal of Hydrology) and the two anonymous reviewers, whose comments improved the original text.

This study was funded by Project CGL2012-35071 of the Spanish Ministry of Economy. One of the authors (JLRB) has a pre-doctoral grant from the University of Lleida.

Contribution of each author

Josep Lluís Ruiz-Bellet: definition of hypotheses, objectives and methodology; sensitivity analysis; calculations with Manning’s equation; writing; figures 1-11; bibliographical research

Xavier Castelltort: definition of objectives and methodology; hydraulic modelling with HEC-RAS and Iber; figures 6-9

J. Carles Balasch: definition of objectives and methodology; document revision

Jordi Tuset: definition of objectives and methodology; hydraulic modelling supervision; document revision

All authors have approved the final article.

References

Abellà, A.: Reconstrucció de les riuades més importants del riu Ebre al seu pas per Móra d'Ebre. Master thesis. University of Lleida, 100 pp, 2013.

Alemseged, T.H. and Rientjes, T.H.M.: Uncertainty issues in hydrodynamic flood modelling. In: Proceedings of the 5th international symposium on spatial data quality SDQ, 2007.

Aronica, G., Hankin, B., and Beven, K.J.: Uncertainty and equifinality in calibrating distributed roughness coefficients in a floods propagation model with limited data. Adv. Water. Resour., 22(4), 349-365, 1998.

Balasch, J.C., Remacha, R., Eritja, X., and Sánchez, A.: 1907. La riuada del Segre a Lleida. Relat històric i interpretació actual. Col·lecció La Banqueta, 36. Pagès Editors, Lleida, 229 pp, 2007.

Balasch, J.C., Ruiz-Bellet, J.L., Tuset, J., and Martín de Oliva, J.: Reconstruction of the 1874 Santa Tecla's rainstorm in Western Catalonia (NE Spain) from flood marks and historical accounts. Nat. Hazards Earth Sys. Sci., 10, 2317-2325, 2010.

Balasch, J.C., Ruiz-Bellet, J.L., and Tuset, J.: Historical flash floods retromodelling in the Ondara River in Tàrrega (NE Iberian Peninsula). Nat. Hazards Earth Sys. Sci., 11, 3359-3371, 2011.

Bales, J.D. and Wagner, C.R.: Sources of uncertainty in flood inundation maps. Journal of Flood Risk Management, 2(2), 139-147, 2009.

Barnolas, M. and Llasat, M.C.: Metodología para el estudio de inundaciones históricas en España e implementación de un SIG en las cuencas del Ter, Segre y Llobregat. CEDEX, Ministerio de Fomento, Monografías M-90, Madrid, 264 pp, 2007.

Barriendos, M. and Coeur, D.: data reconstruction in historical times from non-instrumental sources in Spain and France. In: Benito, G. and Thorndycraft, V.R. (eds.): Systematic, paleoflood and historical data for the improvement of flood risk estimation: Methodological guidelines. CSIC, Madrid, 29-42, 2004.

Barriendos, M., Ruiz-Bellet, J.L., Tuset, J., Mazon, J., Balasch, J.C., Pino, D., and Ayala, J.L.: The Prediflood database of historical floods in Catalonia (NE Iberian Peninsula) AD 1035–2013, and its potential applications in flood analysis. Hydrol. Earth Syst. Sci. 18, 4807-4823, 2014.

Bates, P.D., Anderson, M.G., Hervouet, J.M., and Hawkes, J.C.: Investigating the behavior of two-dimensional finite element models of compound channel flow. Earth Surface Processes and Landforms, 22(1), 3-17, 1997.

Bayliss, A.C. and Reed, D.W.: The Use of Historical Data in Flood Frequency Estimation. Technical Report Report to MAFF, Centre for Ecology and Hydrology, NERC, Wallingford, UK, 2001.

Benito, G., Lang, M., Barriendos, M., Llasat, M.C., Francés, F., Ouarda, T., Thorndycraft, V.R., Enzel, Y., Bardossy, A., Coeur, D., and Bobée, B.: Use of systematic, palaeoflood and historical data for the improvement of flood risk estimation. Review of scientific methods. Nat. Hazards 31, 623-643, 2004.

Benito, G., Brázdil, R., Herget, J., and Machado, M.J.: Quantitative historical hydrology in Europe. Hydrol. Earth Syst. Sci., 19, 3517-3539, 2015.

Beven, K.J.: On undermining the science? Hydrol. Process. (HPToday), 20, 3141-3146, 2006.

Beven, K.J. and Binley, A.M.: The future of distributed models: Model calibration and uncertainty in prediction. Hydrol. Process. 6, 279-298, 1992.

Bladé, E., Cea, L., Corestein, G., Escolano, E., Puertas, J., Vázquez-Cendón, E., Dolz, J., and Coll, A.: Iber: herramienta de simulación numérica del flujo en ríos. Revista

Internacional de Métodos Numéricos para Cálculo y Diseño en Ingeniería, 30(1), 1-10, 2012.

Brázdil, R., Kundzewicz, Z.W., and Benito, G.: Historical hydrology for studying flood risk in Europe. Hydrol. Sci. J. 51, 739-764, 2006.

Bürger, K., Dostal, P., Seidel, J., Imbery, F., Barriendos, M., Mayer, H., and Glaser, R.: Hydrometeorological reconstruction of the 1824 flood event in the Neckar River basin (southwest Germany). Hydrol. Sci. J., 51, 864-877, 2006.

Casas, A., Benito, G., Thorndycraft, V.R, and Rico, M.: La importancia del modelo digital del terreno en modelos hidráulicos de crecidas. In: Benito, G. and Díez-Herrero, A. (eds.): Riesgos naturales y antrópicos en Geomorfología. (Actas de la VIII Reunión Nacional de Geomorfología, Toledo, 22-25 de septiembre de 2004). SEG y CSIC, Madrid, 47-57, 2004.

Cea, L. and Bladé, E.: Modelización matemática en lecho fijo del flujo en ríos. Modelos 1D y 2D en régimen permanente y variable. Jornadas Técnicas sobre Hidráulica Fluvial. Madrid, 3-7 March, 2008.

Chow, V.T.: Open-channel hydraulics. McGraw-Hill, New York, 680 pp, 1959.

Cong, A. and Xu, Y.: Effect of discharge measurement errors on flood frequency analysis. In: Singh, V.P. (ed.): Application of Frequency and Risk in Water Resources. Reidel Publishing Company, 175-190, 1987.

Cowan, W.L.: Estimating hydraulic roughness coefficients. Agricultural Engineering, 37, 473-475, 1956.

Curto, A.: La riuada de 1907. La riuada, 29, 4-8, 2007.

Dawdy, D.R. and Motayed, A.K.: Uncertainties in determination of flood profiles. In: McBean, E.A, Hipel, K.W., Unny, T.E. (eds.): Inputs for risk analysis in water systems. Water Resources Publications, Ft. Collins (USA), 193-208, 1979.

De Roo, A.P.J., Offermans, R.J.E, and Cremers, N.H.D.T.: LISEM: A single-event, physically based hydrological and soil erosion model for drainage basins. II: Sensitivity analysis, validation and application. Hydrol. Process., 10, 1119-1126, 1996.

Di Baldassarre, G. and Montanari, A.: Uncertainty in river discharge observations: a quantitative analysis. Hydrol. Earth Syst. Sci., 13, 913-921, 2009.

Elleder, L.: Reconstruction of the 1784 flood hydrograph for the Vltava River in Prague, Czech Republic. Global Planet. Change 70, 117-124, 2010.

Francés, F.: Flood frequency analysis using systematic and non-systematic information. In: Benito, G. and Thorndycraft, V.R. (eds.): Systematic, paleoflood and historical data for the improvement of flood risk estimation: Methodological guidelines. CSIC, Madrid, 55-70, 2004.

Gallart, F. and Llorens, P.: Observation on land cover changes and water resources in the headwaters of the Ebro catchment, Iberian Peninsula. Phys. Chem. Earth, 29, 769-773, 2004.

Gaume, E., Livet, M., Desbordes, M., and Villeneuve, J.P.: Hydrological analysis of the river Aude, France, flash flood on 12 and 13 November 1999. J. Hydrol. 286, 135-154, 2004.

Ghani A.A.B., Zakaria N.A., Kiat C.C, Ariffin J., Hasan, Z.A., and Ghaffar, A.B.A: Revised equations for Manning's coefficient for Sand-Bed Rivers. International Journal of River Basin Management, 5:4, 329-346, 2007.

Götzinger, J. and Bárdossy, A.: Generic error model for calibration and uncertainty estimation of hydrological models. Water Resour. Res., 44, W00B07, 2008.

Hall, J.W., Tarantola, S., Bates, P.D., and Horritt, M.S.: Distributed sensitivity analysis of flood inundation model calibration. J. Hydraul. Eng., 131(2), 117-126, 2005.

Harmel, R.D., Cooper, R.J., Slade, R.M., Haney, R.L., and Arnold J.G.: Cumulative uncertainty in measured streamflow and water quality data for small watersheds. Trans. Am. Soc. Agric. Biol. Eng., 49(3), 689-701, 2006.

Herget, J. and Meurs, H.: Reconstructing peak discharges for historic flood levels in the city of Cologne, Germany. Global and Planetary Change, 70, 108-116, 2010.

Herget J., Roggenkamp T. and Krelll M., Estimation of peak discharges of historical floods, *Hydrol. Earth Sys. Sc.* **18** (10), 4029-4037

Herget, J., Kapala, A., Krell, M., Rustemeier, E., Simmer, C., and Wyss, A.: The millennium flood of July 1342 revisited. Catena, 130, 82-94, 2015.

Horritt, M.S. and Bates, P.D.: Effects of spatial resolution on a raster based model of flood flow. J. Hydrol., 223, 239-249, 2001.

Horritt, M.S. and Bates, P.D.: Evaluation of 1D and 2D numerical models for predicting river flood inundation. J. Hydrol., 268, 87-99, 2002.

ICGC, Institut Cartogràfic i Geològic de Catalunya: Aerial Photograph. Available at http://www.icc.cat/vissir3/. Last accessed: 27/10/2015.

IGN, Instituto Geográfico Nacional: MDT05/MDT05-LiDAR and MDT25. http://www.ign.es/ign/main/index.do. Last accessed: 12/11/2015.

Jarrett, R.D.: Errors in slope-area computations of peak discharges in mountain streams. J. Hydrol., 96, 53-67, 1987.

Johnson, P.: Uncertainty of hydraulic parameters. J. Hydraul. Eng., 122(2), 112-114, 1996.

Kirby, W.H.: Linear error analysis of slope-area discharge determinations. J. Hydrol., 96, 125-138, 1987.

Lang, M., Fernández-Bono, J.F., Recking, A., Naulet, R., and Grau-Gimeno, P.: Methodological guide for palaeoflood and historical peak discharge estimation. In: Benito, G. and Thorndycraft, V.R. (eds.): Systematic, paleoflood and historical data for the improvement of flood risk estimation: Methodological guidelines. CSIC, Madrid, 43-53, 2004.

Lang, M., Pobanz, K., Renard, B., Renouf, E., and Sauquet, E.: Extrapolation of rating curves by hydraulic modelling, with application to flood frequency analysis. Hydrol. Sci. J., 55(6), 883-898, 2010.

Lenhart, T., Eckhardt, K., Fohrer, N., and Frede, H.-G.: Comparison of two different approaches of sensitivity analysis. Phys. Chem. Earth, 27, 645-654, 2002.

Léonard, J., Mietton, M., Najib, H., and Gourbesville, P.: Rating curve modelling with Manning's equation to manage instability and improve extrapolation. Hydrol. Sci. J., 45(5), 739-750, 2000.

López-Bustos, A.: Antecedentes para una historia de avenidas del río Ebro. Revista de Obras Públicas, 3083, 191-204, 1972.

Lumbroso, D. and Gaume E.: Reducing the uncertainty in indirect estimates of extreme flash flood discharges. J. Hydrol., 414, 16-30, 2012.

Machado, M.J., Botero, B.A., López, J., Francés, F., Díez-Herrero, A., and Benito, G.: Flood frequency analysis of historical flood data under stationary and non-stationary modelling. Hydrol. Earth Syst. Sci., 19, 2561-2576, 2015.

MAGRAMA, Ministerio de Agricultura, Alimentacion y Medio Ambiente: Anuario de aforos. Available at http://sig.magrama.es/aforos/visor.html. Last accessed: 18/11/2015.

Marcus, W.A., Roberts, K., Harvey, L., and Tackman, G.: An evaluation of methods for estimating Manning's n in small mountain streams. Mountain Research and Development, 12(3), 227-239, 1992.

Martín-Vide, J.P.: Ingeniería de ríos. Edicions UPC, Barcelona, 404 pp, 2002.

McCuen, R.H.: The role of sensitivity analysis in hydrologic modelling. J. Hydrol., 18, 37-53, 1973.

Mérida, D.: Estudi comparatiu del model Iber amb el model HEC-RAS per a l'avinguda histórica de 1907 al riu Ebre en Benifallet (Baix Ebre). Master's degree thesis, University of Lleida, 87 pp, 2014.

Merwade, V., Olivera, F., Arabi, M., and Edleman, S.: Uncertainty in Flood Inundation Mapping: Current Issues and Future Directions. J. Hydrol. Eng., 13(7), 608-620, 2008.

Miravall, R.: Flagells naturals sobre Tortosa. Riuades, gelades, aiguats i sequeres, ventades i terratrèmols. Columna, Barcelona, 191 pp, 1997.

Montanari, A.: What do we mean by “uncertainty”? The need for a consistent wording about uncertainty assessment in hydrology. Hydrol. Proc., 21, 841-845, 2007.

Naulet, R., Lang, M., Ouarda, T.B., Coeur, D., Bobée, B., Recking, A., and Moussay, D.: Flood frequency analysis on the Ardèche river using French documentary sources from the last two centuries. J. Hydrol. 313, 58-78, 2005.

Neppel, L., Renard, B., Lang, M., Ayral, P.A., Coeur, D., Gaume, E., Jacob, N., Payrastre, O., Pobanz, K., and Vinet, F.: Flood frequency analysis using historical data: accounting for random and systematic errors. Hydrol. Sci. J., 55, 192-208, 2010.

Nicholas, A.P. and Walling, D.E.: Numerical modelling of floodplain hydraulics and suspended sediment transport and deposition. Hydrol. Process., 12(8), 1339-1355, 1998.

O’Connor, J.E. and Webb, R.H.: Hydraulic modelling for paleoflood analysis. In: Baker, V.R. and Patton, P.C. (eds.): Flood geomorphology. John Miley & Sons, New York, 393-402, 1988.

Pappenberger, F. and Beven, K.J.: Ignorance is bliss: Or seven reasons not to use uncertainty analysis. Water Resour. Res., 42, W05302, 2006.

Pappenberger, F., Beven, K.J., Horritt, M., and Blazkova, S.: Uncertainty in the calibration of effective parameters in HEC-RAS using inundation and downstream level observations. J. Hydrol., 302, 46-69, 2005.

Pappenberger, F., Matgen, P., Beven, K.J., Henry, J.B., Pfister, L., and de Fraipont, P.: Influence of uncertain boundary conditions and model structure on flood inudation predictions. Adv. Water Resour., 29, 1430-1449, 2006.

Paquier, A. and Mignot, E.: Use of 2D models to calculate flood water levels: calibration and sensitivity analysis. In: Ganoulis, J. and Prinos, P. (eds.): XXX IAHR Congress, Thessaloniki, 24-29, 2003.

Payrastre, O., Gaume, E., and Andrieu, H.: Usefulness of historical information for flood frequency analyses: Developments based on a case study. Water Resour. Res. 47, W08511, 2011.

Pelletier, M.P.: Uncertainties in the determination of river discharge: a literature review. Can. J. Civ. Eng., 15, 834-850, 1988.

Pino, D., Ruiz-Bellet, J.L., Balasch, J.C., Romero-León, L., Tuset, J., Barriendos, M., Mazón, J., and Castelltort, X.: Meteorological and hydrological analysis of major floods in NE Iberian Peninsula. Journal of Hydrology, 541 (A), 63-89, 2016.

Quick, M.C.: Reliability of flood discharge estimates. Can. J. Civ. Eng., 18(4), 624-630, 1991.

Refsgaard, J.C., van der Sluijs, J.P., Brown, J., and van der Keur, P.: A framework for dealing with uncertainty due to model structure error. Adv. Water Resour., 29, 1586-1597, 2006.

Remo, J.W.F. and Pinter, N.: Retro-modeling the middle Mississippi River. J. Hydrol., 337, 421-435, 2007.

Ruiz-Bellet, J.L., Balasch, J.C., Tuset, J., Barriendos, M., Mazón, J., and Pino, D.: Historical, hydraulic, hydrological and meteorological reconstruction of 1874 Santa Tecla flash floods in Catalonia (NE Iberia Peninsula). J. Hydrol., 524, 279-295, 2015a.

Ruiz-Villanueva, V., Díez-Herrero, A., Stoffel, M., Bollschweiler, M., Bodoque, J.M., and Ballesteros, J.A.: Dendrogeomorphic analysis of flash floods in a small ungauged mountain catchment (Central Spain). Geomorphol., 118, 383-392, 2010.

Sánchez, A.: Modelización hidráulica y análisis de magnitud-frecuencia de avenidas históricas en el curso bajo del Rio Ebro. Master’s degree thesis, University of Lleida, 77 pp., 2007.

Sauer, V.B. and Meyer, R.W. (1992): Determination of error in individual discharge measurements. USGS Open File Report 92-144. Washington, D.C.

Schmidt, A.R.: Analysis of stage-discharge relations for open channel flow and their associated uncertainties. PhD thesis. University of Illinois, Urbana, 328 pp., 2002.

Schumann, G., Cutler, M., Black, A., Matgen, P., Pfister, L., Hoffmann, L., and Pappenberger, F.: Evaluating uncertain flood inundation predictions with uncertain remotely sensed water stages. International Journal of River Basin Management, 6(3), 187-199, 2008.

Tuset, J.: Reconstrucció de l'aiguat de Santa Tecla (23 de setembre de 1874) en el riu Sió a Mont-Roig a partir de documentació histórica. Master's degree thesis, University of Lleida, 40 pp., 2011.

USACE, US Army Corps of Engineers (ed.): HEC-RAS River Analysis System Version 4.1. User's Manual. US Army Corps of Engineers Hydrologic Engineering Center, Davis, 790 pp., 2010.

Van Griensven, A., Meixner, T., Grunwald, S., Bishop, T., Diluzio, M., and Srinivasan, R.: A global sensitivity analysis tool for the parameters of multi-variable catchment models. J. Hydrol., 324, 10-23, 2006.

Vericat, D. and Batalla, R.J.: Sediment transport in a large impounded river: the lower Ebro River (NE Iberian Peninsula). Geomorphology, 79, 72-92, 2006.

Wilson, M.D.: Evaluating the Effect of Data and Data Uncertainty on Predictions of Flood Inundation. University of Southampton, Southampton, 276 pp., 2004.

Wohl, E.E.: Uncertainty in flood estimates associated with roughness coefficient. J. Hydraulic Eng., 124(2), 219-223, 1998.

Zadeh, L.A.: Toward a generalized theory of uncertainty (GTU)—an outline. Inform. Sciences, 172, 1-40, 2005.

Table 1. Previous estimates of peak flows of 1907 flood and survey of the damages that it caused in different locations (see Fig. 1).

Town	River	Reconstructed peak flow		Deaths and damages	
		Value ($m^3 \cdot s^{-1}$)	Source	Count	Source
Lleida	Segre	5250[a]	Balasch et al., 2007	Bridge, embankment and 300–400 dwellings destroyed	Balasch et al., 2007
Móra d'Ebre	Ebro	11200[a]	Abellà, 2013	More than 50 buildings destroyed	Curto, 2007
Benifallet	Ebro	11500[a] 10000[b]	Mérida, 2014	5 buildings destroyed	Curto, 2007
Xerta	Ebro	10500[a,c]	Sánchez, 2007	2 buildings destroyed	Curto, 2007
Tivenys	Ebro			23 buildings destroyed	
Tortosa	Ebro	12000[d]	López-Bustos, 1972	3 deaths and 7 buildings destroyed	Miravall, 1997; Curto, 2007

[a] Calculated with the HEC-RAS model (one-dimensional).

[b] Calculated with the Iber model (two-dimensional).

[c] Recalculated in Sect. 4.1.

[d] Estimated with unspecified methods.

Table 2. Values of the input variables used in the peak flow reconstruction of 1907 flood with HEC-RAS

Input variable			Value
1907 flood mark from flood scale at 1, Major Square, Xerta		X[a]	288,655
		Y[a]	4,531,394
		z (m a.s.l.)	15.175
1907 flood mark at 1, Major Street, Xerta		X[a]	288,714
		Y[a]	4,531,407
		z (m a.s.l.)	15.325
1961 flood mark from flood scale at 1, Major Square, Xerta		X[a]	288,655
		Y[a]	4,531,394
		z (m a.s.l.)	12.171
1961 peak flow ($m^3 \cdot s^{-1}$); source MAGRAMA (2015)			4580
Manning's n			Calibrated with 1961 flood (See Table 5)
Length of the modelled reach (m)			7690
HEC-RAS specific parameters	Number of cross sections		45
	DEM resolution (m); source IGN (2015)		5x5
	Boundary conditions	Upstream	Critical depth
		Downstream	Normal depth[b]: 0.905 $m \cdot km^{-1}$
	Contraction/expansion coefficients[c]		0.1/0.3
	Type of flow		Steady mixed

[a] UTM coordinates: reference frame ETRS89, zone 31T

[b] When "Normal depth" is chosen as the downstream boundary condition in the HEC-RAS, a water surface slope is asked; for the sake of simplicity, we considered the water surface parallel to the channel's bottom: 0.0905 $m \cdot m^{-1}$ is the slope of the channel.

[c] Default values used by HEC-RAS.

Table 3. Hydrograph used in the hydraulic modelling with Iber

Time (s)	Flow ($m^3 \cdot s^{-1}$)
0	2000
7200	12500
14400	8000
28800	6000

Table 4. The five hydraulically homogeneous sectors into which the flood scale cross section was divided in one of the three methods of division in order to apply the Manning's equation, with their characteristics.

Sector		Position in the x axis in Fig. 8 (m)	Wetted area (m^2)	Wetted perimeter (m)	Average Manning's n[a] ($s \cdot m^{-1/3}$)	Longitudinal slope ($m \cdot km^{-1}$)
Left floodplain		4–412	2059	413	0.051	1
Channel		412–545	1386	135	0.041	1
Right floodplain	Not urban	545–707	736	132	0.047	1
	Urban	707–1003	913	287	0.092	1
	Not urban	1003–1232	410	218	0.058	1
Total		4–1232	5504	1212	0.060	---

[a] Average Manning's n weighted by wetted perimeter of each soil use in the flood scale cross section. Manning's n values calibrated with 1961 flood (Table 5).

Table 5. Manning's n values calibrated with 1961 flood for the soil uses identified in Fig. 6, compared to those calibrated by Sánchez (2007) with the same flood and to the general values given by Chow (1959) and Martín-Vide (2002)

Soil use	Area within the flooded part of the flood scale cross section[(a)] (km^2)	Manning's n general values (Chow, 1959) ($s \cdot m^{-1/3}$)	Manning's n values in this study			Sánchez (2007)	Relative differ-ence[(c)] (%)
			Initial values ($s \cdot m^{-1/3}$)	Values calibrated with 1961 flood ($s \cdot m^{-1/3}$)	Relative differ-ence[(b)] (%)	Manning's n values calibrated with 1961 flood ($s \cdot m^{-1/3}$)	
Channel	1.28	0.031–0.100	0.035	0.041	+16	0.038, 0.040	+2, +8
Canals	0.18	0.030	0.030	0.030	0	No data	---
Bare floodplain	0.30	0.030–0.050	0.050	0.048	–4	No data	---
Vegetated floodplain (shrubs)	0.46	0.045–0.100	0.060	0.060	0	0.100	–50
Riparian forest	0.01	0.080–0.160	0.085	0.085	0	0.100	–16
Crops and orchards	2.60	0.030–0.050	0.050–0.060	0.050	0, –10	No data	---
Olive and almond trees	0.05	0.050–0.080	0.065	0.065	0	0.060	+8
Roads	0.06	0.016	0.050	0.050	0	No data	---
Urban area	0.12	0.100[(d)]	0.100	0.100	0	0.030	+108
Total	5.06	---	0.050[(e)]	0.049[(e)]	–2.3	0.060[(f)]	–20

[(a)] Major Square's flood scale cross section

[(b)] Relative difference (Rd) calculated as: $Rd = \frac{n_1 - n_2}{\frac{n_1 + n_2}{2}} \cdot 100$, where n_1 is the calibrated Manning's n used in this study and n_2 is the initial one.

[(c)] Relative difference (Rd) calculated as: $Rd = \frac{n_1 - n_2}{\frac{n_1 + n_2}{2}} \cdot 100$, where n_1 is the calibrated Manning's n used in this study and n_2 is the one used by Sánchez (2007).

[(d)] Martín-Vide (2002); Chow (1959) provided no value for urban areas

[(e)] Average Manning's n weighted by area of each soil use within the flooded part of the modelled reach.

[(f)] Urban area (streets) not taken into account because considered hydraulically ineffective.

Table 6. Results of the hydraulic reconstruction of 1907 flood in Xerta

Variable	Observed	Modelled with a peak flow of 11500 $m^3 \cdot s^{-1}$	Difference (cm)
Water height at Major Square's flood scale (m)	15.175	15.17	–0.5
Water height at Major Street's flood mark (m)	15.325	15.33	+0.5

Table 7. Results of the use of Manning's equation at the flood scale cross section, depending on the number of sectors into which the cross section was divided

Method (Number of sectors into which the cross section was divided)	Sector		Peak flow ($m^3 \cdot s^{-1}$)
5	Left floodplain		3744
	Channel		5056
	Right floodplain	Not urban	1353
		Urban	677
		Not urban	342
	Total		11172
17	---		11534
276	---		11759

Table 8. The 14 sensitivity analyses performed and their results

Sensitivity analyses				Influence on the peak flow			
Number	Modified input variable	Initial value	Modification of the initial value	Resulting peak flow ($m^3 \cdot s^{-1}$)	Absolute individual error ($m^3 \cdot s^{-1}$)	Relative individual error (%)	Sensitivity index (I_x)
1	Water height at the flood scale cross section	15.175 m a.s.l.	+10 cm	11750	±275	±2.4	+3.6
2			–10 cm	11200			
3			+30 cm	12325	±838	±7.3	+3.7
4			–30 cm	10650			
5			+100 cm	14430	±2803	±24.4	+3.7
6			–100 cm	8825			
7	Manning's n	A different one for each cross section, according to soil uses (see Table 5)	+30%	8925	±3500	±30.4	–1.0
8			–30%	15925			
9			Channel: 0.045 (+9%) Floodplain: 0.056 (+7%) Average [b]: 0.055 (+8%)	10225	–1275	–11	–1.4
10	Downstream boundary condition: normal height[c]	0.905 $m \cdot km^{-1}$	+15%	11880	±455	±4.0	+0.3
11			–15%	10970			
12	Number of cross sections	45	22	14330	+2830	+25	+0.5
13	Flow paths direction (Fig. 8)	Straight	Meandering	11500	0	0	NA[d]
14	DEM resolution	5x5	25x25	11475	–25	–0.2	+0.01

[a] Major Square's flood scale cross section

[b] Average Manning's n weighted by area of each soil use in the flooded part of the modelled reach.

[c] When "Normal height" is chosen as the downstream boundary condition in the HEC-RAS, a water surface slope is asked; for the sake of simplicity, we considered the water surface parallel to the channel's bottom: 0.0905 $m \cdot m^{-1}$ is the slope of the channel downstream the modelled reach.

[d] NA: not applicable, because "straight" and "meandering" cannot be expressed in numbers to calculate Eq. (5).

Table 9. Peak flow total error (relative and absolute) and the relative contribution to it of the five variables with a sensitivity index above zero, depending on the water height uncertainty considered and on the inclusion in the calculation or not of the error caused by the reduction of the number of cross sections

Error caused by the reduction of the number of cross sections	Water height uncer-tainty considered (cm)	Peak flow total absolute error [a] ($m^3 \cdot s^{-1}$)	Peak flow total relative error [a] (%)	Relative contribution to the peak flow total error [a] (%)				
				Water height	Manning's n	Down-stream boundary condition	Number of cross sections	DEM reso-lution
Not included	±10	±3540	±31	6	82	11	NA[b]	<1
	±30	±3627	±32	17	73	9	NA[b]	<1
	±100	±4507	±39	41	52	7	NA[b]	<1
Included	±10	±4532	±39	4	49	6	40	<1
	±30	±4601	±40	11	46	6	37	<1
	±100	±5322	±46	29	36	5	29	<1

[a] Calculations do not take into account the error found in sensitivity analysis 9, because it is included in the error found in sensitivity analysis 8 (see Sect. 4.3.2).

[b] NA: Not applicable, because the error caused by the reduction of the number of cross section is not taken into account

Table 10. Comparison of Manning's n sensitivity indexes from different studies

Source	Δ_n Manning n variation (%)	δ_n Peak flow relative error (%)	Sensitivity index ($I_x=\delta_n/\Delta_n$)	Model used	Observations
De Roo et al. (1996)	±20	±15	−0.8	LISEM	Erosion model
Wohl (1998)	±25	±20	−0.8	HEC-2	In canyon rivers with a longitudinal slope smaller than 0.01 $m \cdot m^{-1}$
Naulet et al. (2005)	±20	±10	−0.5	MAGE	In large floods in the Ardèche River
Di Baldassarre and Montanari (2009)	+33	−7	−0.2	HEC-RAS	In a range of high flows between 10000 and 12000 $m^3 \cdot s^{-1}$ in the Po River in Pontelagoscuro
Herget and Meurs, 2010	±25	±21	−0.9	Manning's equation	In 1374 flood in the River Rhine in Collogne
Herget et al. (2015)	±9 and ±26	±9 and ±27	−1.0 and −1.1	Manning's equation	In 1342 flood in the Main River in Würzburg (2 hydraulic scenarios)
Ruiz-Bellet et al. (2015a)	±30	±5 to ±11	−0.2 to −0.4	HEC-RAS	In four hydraulic reconstructions in streams with small catchments (150–314 km^2)
This study	±30	±30	−1.0	HEC-RAS	In 1907 flood in Ebro River in Xerta

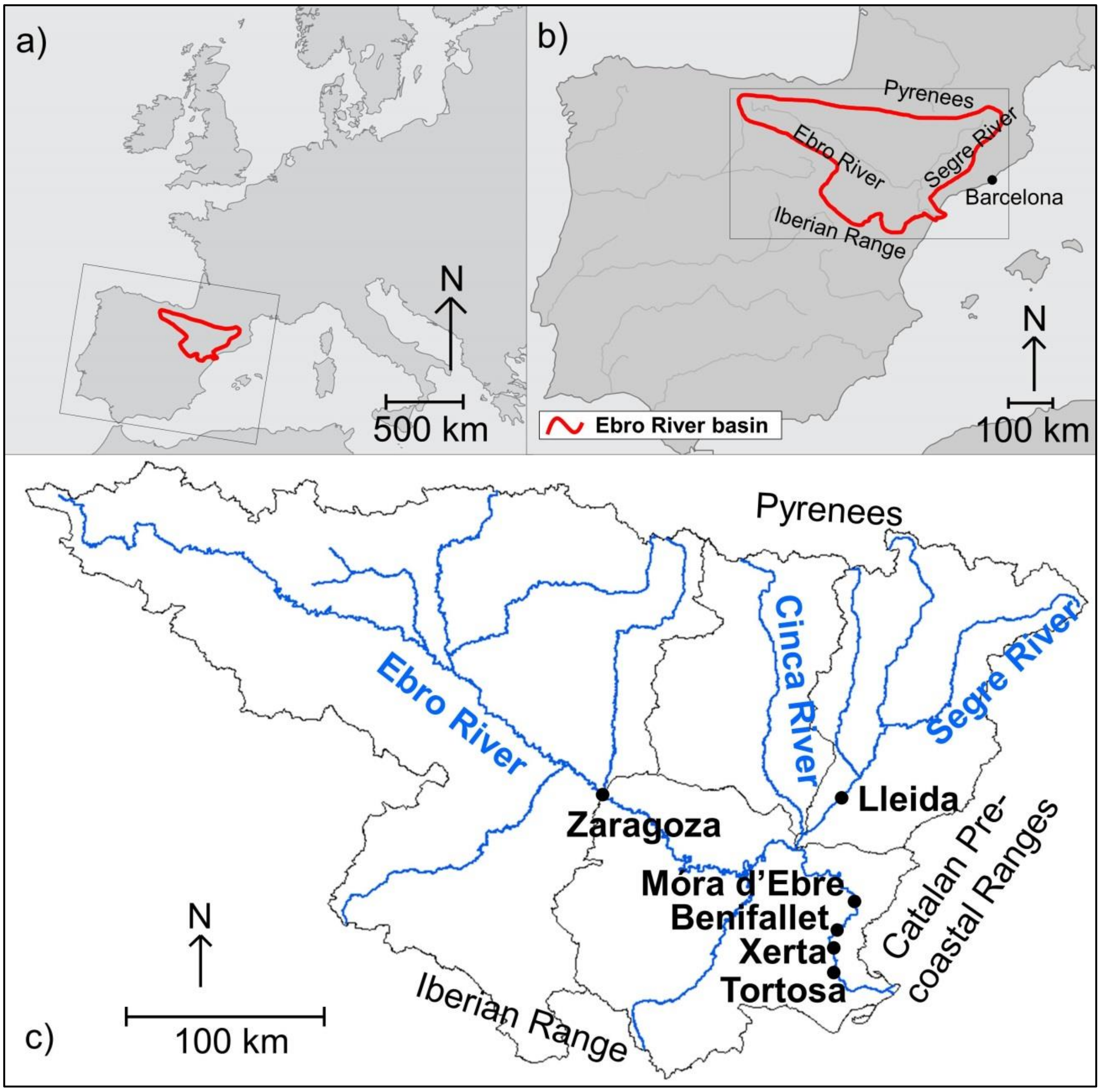

Figure 1. Location of the Ebro basin within Europe (a) and the Iberian Peninsula (b), and of the town of Xerta within the Ebro basin (c). Maps (a) and (b) modified from a map Copyright © 2009 National Geographic Society, Washington, D.C.; map (c) drawn by Damià Vericat (RIUS-University of Lleida).

Figure 2. The towns of Xerta and Tivenys on either sides of a meander of the Ebro River. Adapted from an aerial photograph of June 2014 (ICGC, 2015).

Figure 3. Flood scale on the façade of the Assumption Church at 1, Major Square in Xerta (Photo by Alberto Sánchez)

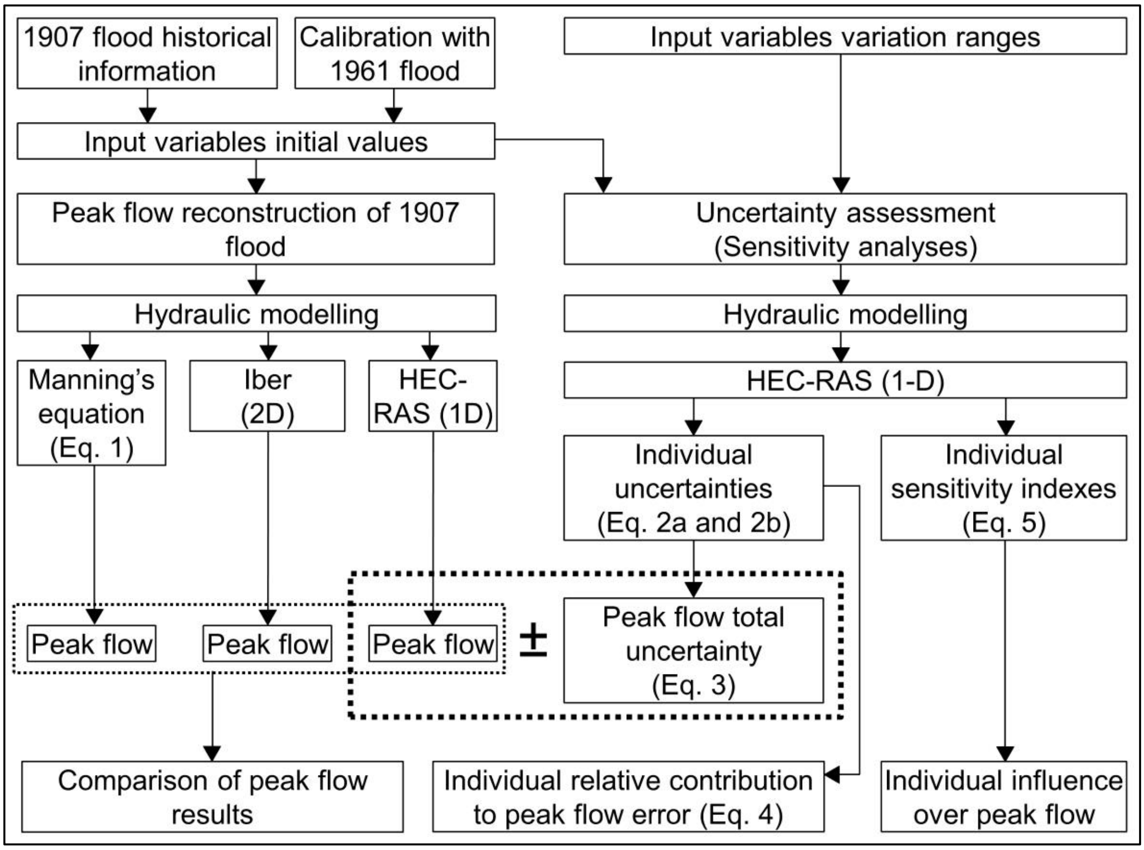

Figure 4. Overview of the methodological procedure

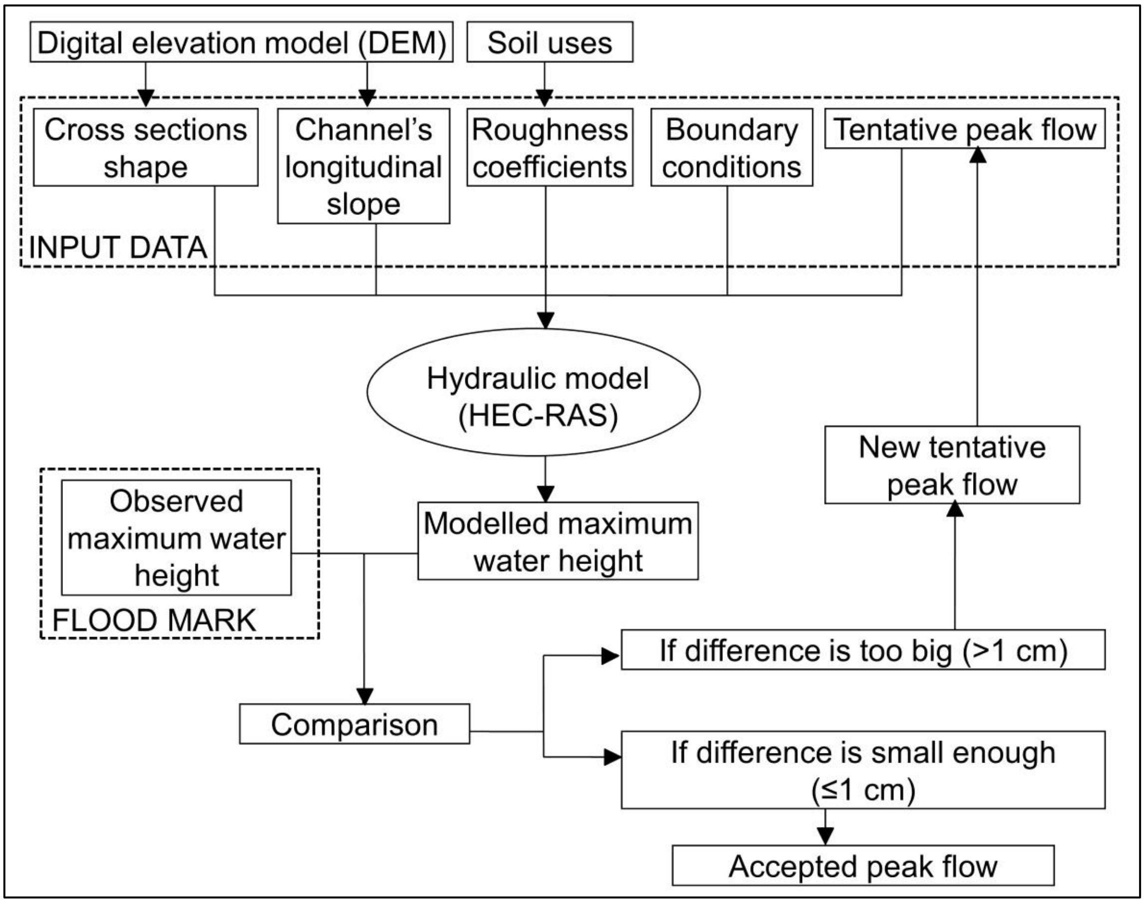

Figure 5. Peak flow reconstruction procedure with the hydraulic model HEC-RAS (Adapted from Balasch et al., 2010)

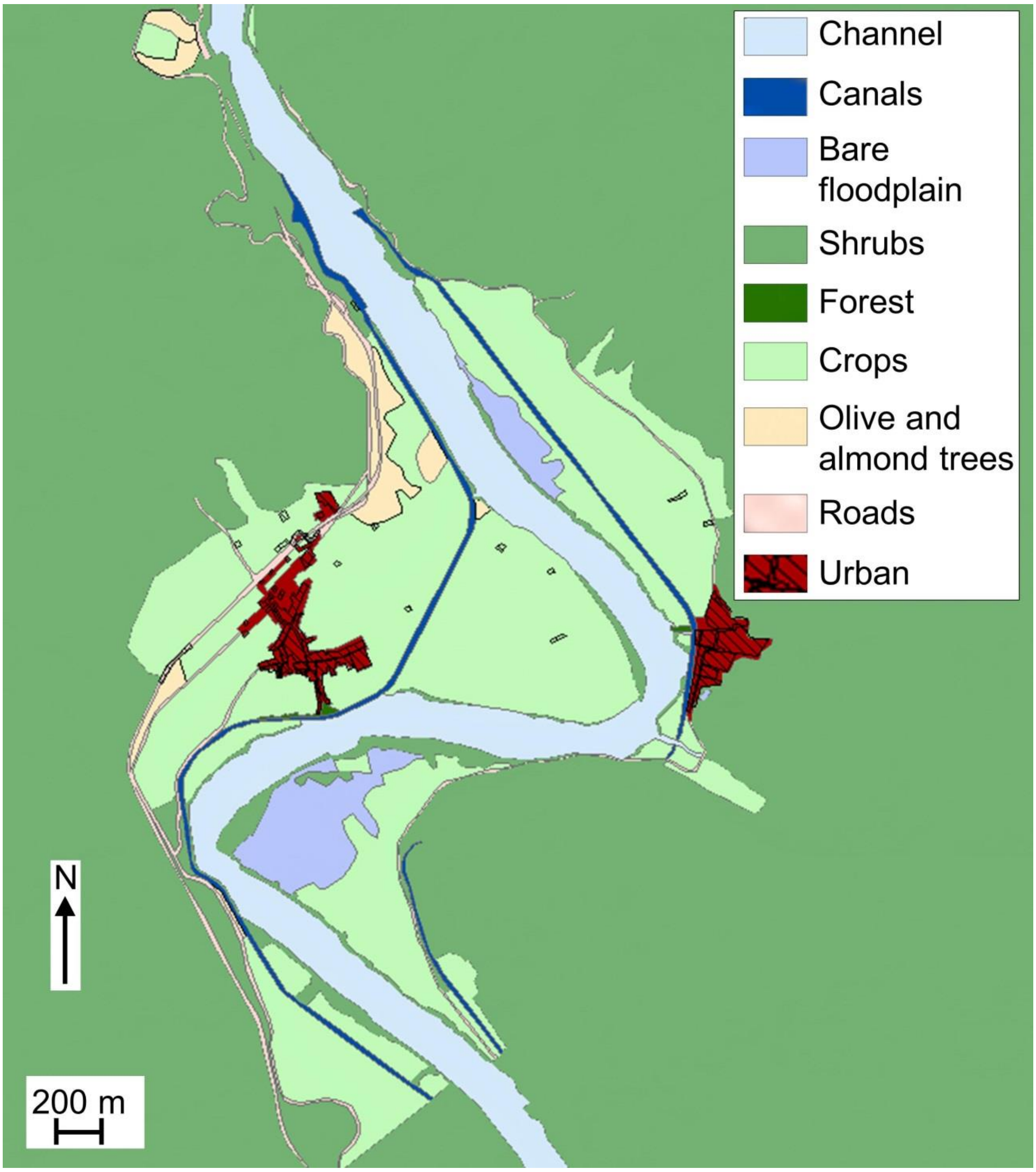

Figure 6. Soil uses determined from aerial photographs of 1957. (Source: ICGC, 2015)

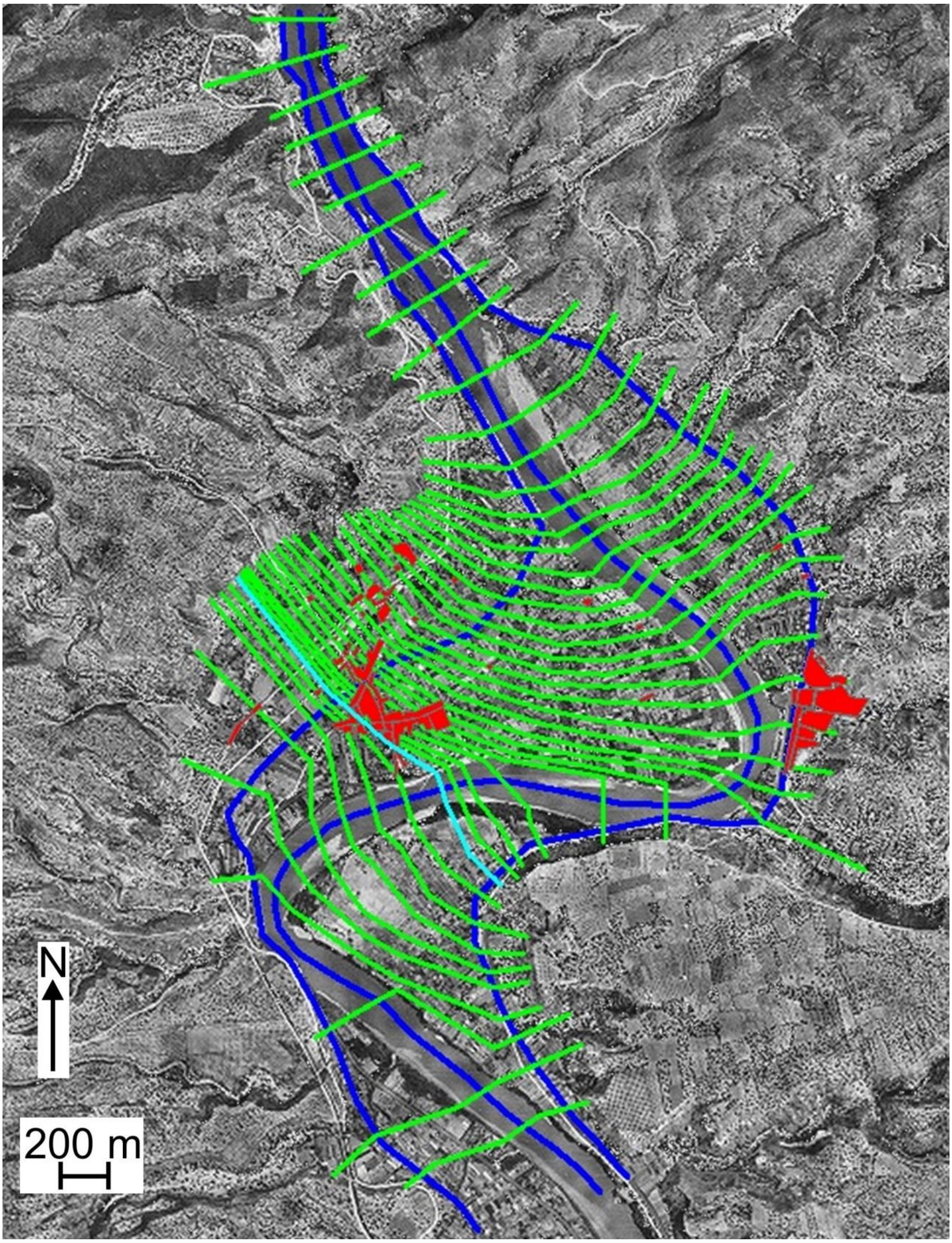

Figure 7. Modelled reach with the cross sections (green lines), flow paths (blue lines) and the towns (red areas) of Xerta (left) and Tivenys (right), superimposed over an orthophotograph of ICGC (2015).

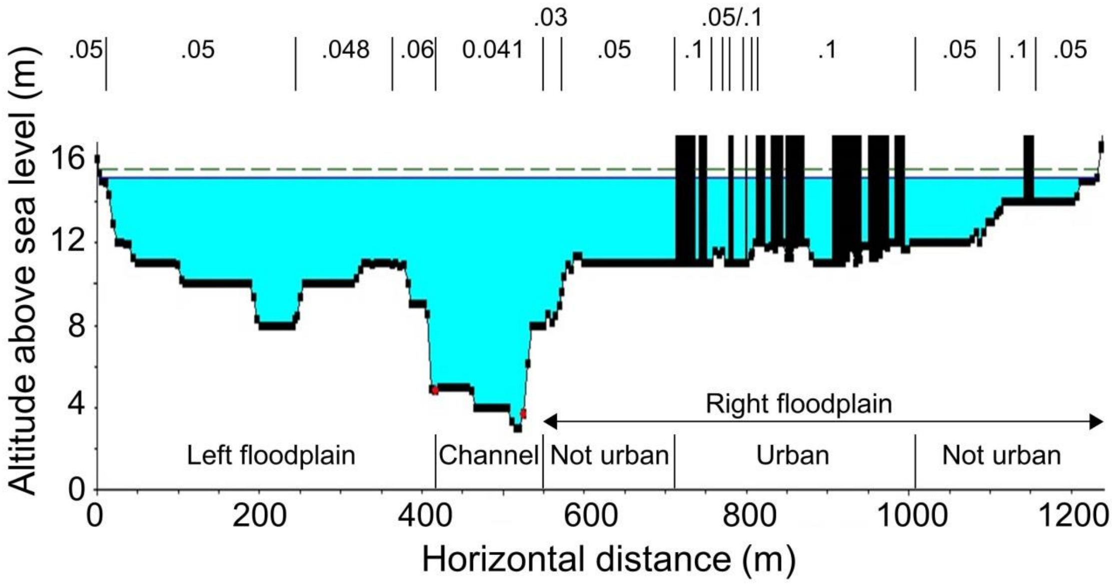

Figure 8. The flood scale cross section, with the three methods of dividing it: the five hydraulically homogeneous sectors (labelled near the horizontal axis); the 17 sectors into which it was divided according to the soil use, each one with its Manning's n value (above the cross section); the 276 sectors into which HEC-Geo-RAS divided the cross section (limited by the 277 black rectangular dots over the line that outlines the cross section).

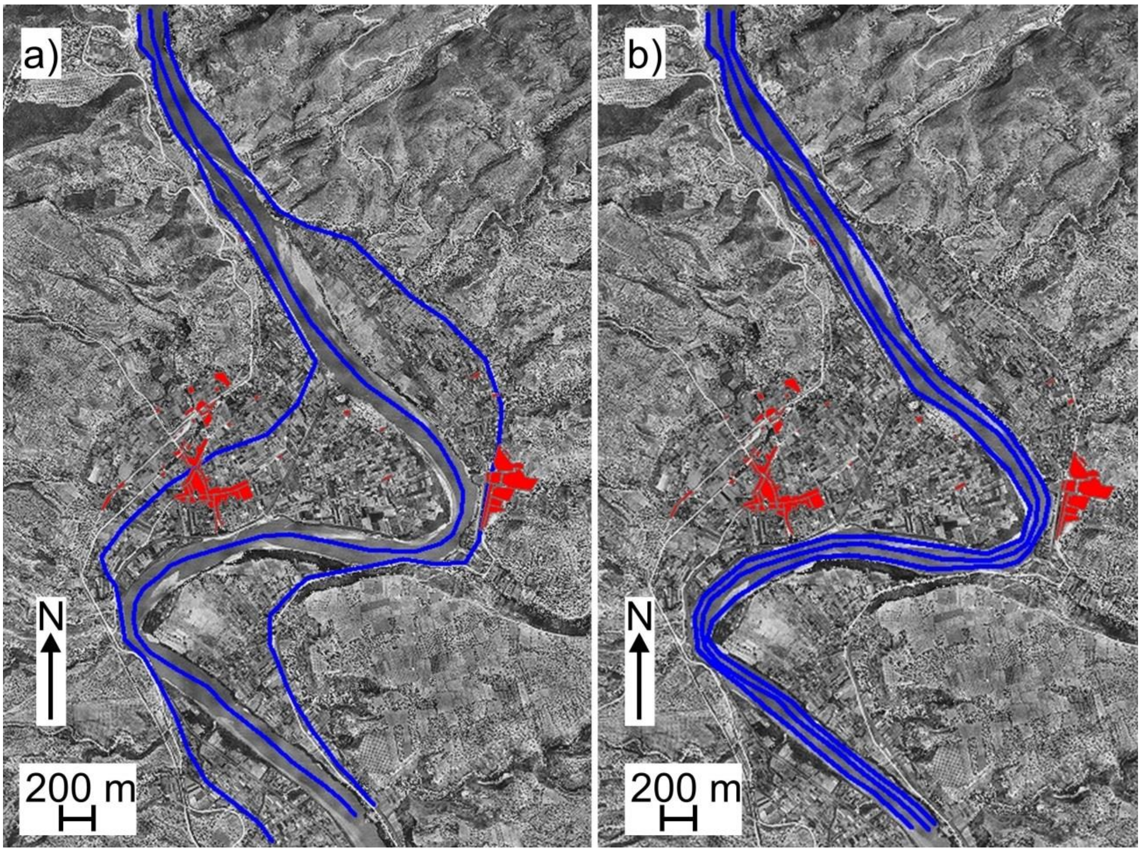

Figure 9. Two ways of drawing the flow path lines required in the HEC-RAS programme: (a) straight and (b) meandering

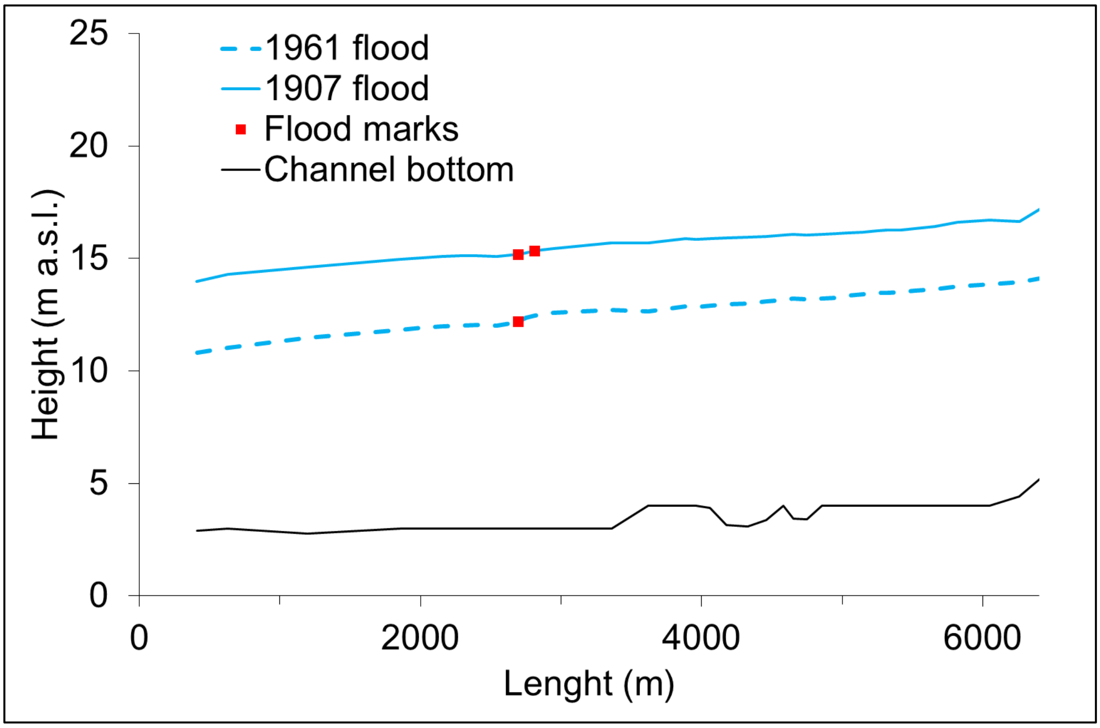

Figure 10. Modelled longitudinal water profiles of 1907 and 1961 floods and the three flood marks used

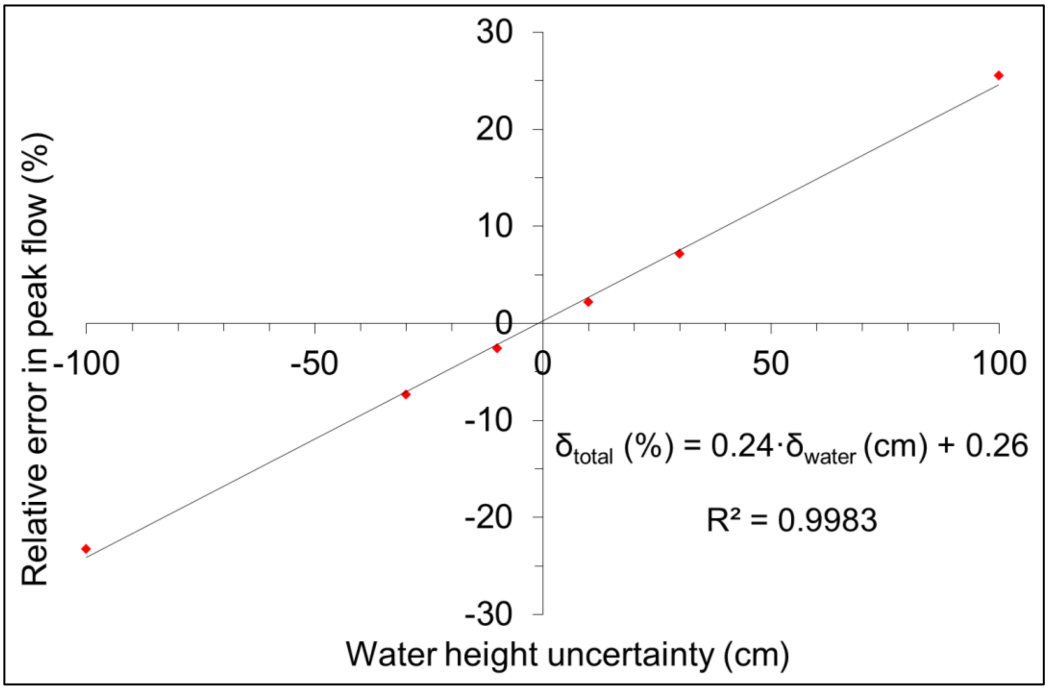

Figure 11. Relative error in the modelled peak flow of 1907 flood in Xerta, caused by the six water height uncertainties tested